2009

Characterization and transitions of asphalt cement composite materials

Brent Harper Sellers
Louisiana State University and Agricultural and Mechanical College, bselle4@tigers.lsu.edu

CHARACTERIZATION AND TRANSITIONS OF ASPHALT CEMENT COMPOSITE MATERIALS

A Thesis

Submitted to the Graduate Faculty of
Louisiana State University and
Agricultural and Mechanical College
in Partial Fulfillment of the
Requirements for the Degree of
Master of Science

in

The Department of Chemistry

By
Brent H. Sellers
B. S., University of North Carolina at Charlotte, 1999
August, 2009

TABLE OF CONTENTS

LIST OF TABLES

LIST OF FIGURES

ABSTRACT

Blends of a PG 64-22 asphalt with a range of load levels (0.2 — 20 wt %) of Sasobit® wax and a single loading of 2 wt % Elvaloy AM® were prepared and characterized. Sasobit® wax is a high molecular weight paraffinic wax produced commercially through the Fischer-Tropsch process. Elvaloy AM® is a reactive elastic terpolymer, comprised of ethylene, butyl acrylate and glycidyl methacrylate monomeric units. The blends were analyzed by gel permeation chromatography (GPC), differential scanning calorimetry (DSC), x-ray diffraction, epifluorescence microscopy, scanning laser confocal microscopy, and dynamic shear rheology. Sasobit (1 wt %) composite material showed little difference in aging characteristics with respect to the aging chromatograms of the un-modified asphalt cement. Aging of Elvaloy (2 wt %) composite material leads to increased concentrations of asphaltene and asphaltene aggregate components at a greater rate than that observed with the Sasobit composites and unmodified asphalt cement. Analysis of DSC heating curve enthalpies revealed that Sasobit composites at loadings above 4% that the Sasobit was completely crystalline. X-ray diffraction confirmed that ambient temperature Sasobit composite samples maintained their crystalline form down to the level of 0.2 wt % loading. Evidence for the additives presence could be seen within the asphalt matrix through epifluorescence and scanning laser confocal microscopy imaging of each of the composite systems investigated. Bright point-sources of fluorescence, most easily picked out in the Elvaloy (2 wt %) composite images, are believed to be asphaltene micelles. Evidence of improved G* performance in both Sasobit and Elvaloy composite master curves with respect to the neat asphalt cement master curves is presented. The dynamic viscosity data at 1 Hz shows that original and TFOT data doesn't clearly differentiate between Sasobit composites and neat asphalt cement until after PAV aging. At that stage the

Sasobit composite shows truly linear dynamic viscosity response suggesting that Sasobit inclusion leads to better dispersion of the viscosity building asphaltene component throughout the asphalt cement. It is believed that the Elvaloy AM composite experienced some degree of crosslinking during aging and this is most evident following the PAV aging in the rheological data.

CHAPTER 1

INTRODUCTION

1.1 Background

Within this thesis there are two different asphalt cement grading systems discussed, the viscosity grading system (AC) and the currently employed performance grading system (PG). The viscosity grading (AC) system is based on the viscosity of the asphalt cement in its original or un-aged form and the specifications can be found in ASTM D3381.[1] The viscosity grading system is based on the measured asphalt cement viscosity in poise (P) at 60 ^{o}C and ranges from AC-2.5 (250P) to AC-70 (7000P). This grading system was found to be deceptive since the asphalt cement was not graded in terms of its required in-service performance.[2]

In 1987, the Strategic Highways Research Program (SHRP) was initiated to develop new testing protocols for grading asphalt cement in terms of its resistance to rutting, fatigue cracking and thermal cracking. The performance grading system specifications, also referred to as the Superpave® (**Su**perior **Per**forming Asphalt **Pave**ments) specifications, can be found in AASHTO MP1.[3] The performance grading system (PG) specifies the average 7-day ambient pavement high temperature as the first value, followed by the minimum environmental pavement temperature to be experienced in-service. For example, a PG 64-22 asphalt cement is intended for an environment in which the 7-day average maximum pavement temperature is not to exceed 64 ^{o}C and the minimum expected pavement temperature is not expected to be lower than -22 ^{o}C. The maximum pavement temperature states that this asphalt cement will be stiff enough to resist rutting below that temperature, while the minimum temperature states that the material will be elastic and strong enough to be able to resist low temperature cracking down to that temperature value.[3]

Pg 64-22 (Marathon Oil Corp) was chosen as the asphalt cement mixed with the additives to form the composites investigated in this study. This grade of asphalt cement is produced without any polymeric reinforcement. Neat asphalt cement is a colloidal system consisting of a rigid multi-aromatic ring structured asphaltene discontinuous phase, dispersed in a lower molecular mass maltene continuous phase. The percentage of asphaltenes in asphalt cement is approximately 29 % or less, depending on the asphalt cement source.[5b] The asphaltene phase is more polar than the maltenes phase and has reactive functional groups through which it can form aggregates with itself or form bonds to stone aggregate and reactive functional groups on some reinforcing additives. The asphaltene phase has the most influence over the system viscosity in asphalt cement.[2]

Corbett reported that when asphalt cement is dissolved in *n*-heptane (at 100 ^{o}C), the asphaltene fraction will precipitate out and can be separated through filtration using filter paper, leaving the maltene potion of the asphalt cement sample in solution with *n*-heptane.[5a] The asphaltenes appear as brown to black solid. The recovered solution was further fractionated using an alumina filled chromatographic column. Two of the three fractions making up the maltene portion will absorb to the alumina. When excess *n*-heptane is run through the column the saturated fraction will elute, leaving a colorless liquid upon removal of the solvent. Benzene is then used as the elution solvent for the naphthalene-aromatic fraction and will appear as a yellow to red liquid upon removal of the solvent. The final polar-aromatic fraction can be eluted using a 50 % methanol/benzene solution followed by excess trichloroethylene. When the solvents are removed, the polar-aromatic fraction will be a black solid. This method has been adopted with some changes by the American Society for Testing and Materials as ASTM D4124.[5b]

Unmodified asphalt cement as a paving material has been used for more than 100 years. While there are naturally occurring deposits in areas of the world in which pools of asphalt cement can be found, most of the asphalt cement used in paving projects is derived through the processing of crude oil residue.[3] Asphalt cement is also referred to as bitumen and asphalt binder in publications and must be differentiated from hot mix asphalt (HMA) or mixture which specifies that asphalt cement has been mixed with stone aggregate and sand. The distresses of unmodified asphalt cement such as embrittlement with age, low temperature cracking, fatigue cracking and rutting at high temperature curtail its use in many of today's roadways and other paving applications.[6] In order to reduce the influence of these distresses, various performance enhancing additives are added to asphalt cement to improve the performance of pavement and give longer service life.[7-9] Since 1994 the Louisiana Department of Transportation has used polymer modified asphalt cement in the majority its hot mix asphalt cement paving projects.[10] These projects are now coming due for re-paving and new technologies such as warm mix asphalt (WMA) may be utilized in the pavement construction.[11, 12]

Conventional hot mix asphalt production takes place between 120-163 ^{o}C and placement followed by compaction occurs in the range of 130-150 ^{o}C. During the production and construction period, the asphalt cement experiences the greatest oxidation rate it will experience over its service life.[2] If the temperature the asphalt cement experiences during production and construction can be reduced, there will be a lower initial oxidation rate which can lead to longer paving service life and better overall pavement performance.

The use of WMA technology can result in a reduction of asphalt cement production temperature by an estimated 40 %.[12, 13] The reduced production temperature cost savings can be realized by the production contractor in the form of an approximately 30 % reduction in fuel consumption.[13] Along with the reduced production temperature

and the fuel consumption the emissions of odor and greenhouse gasses will also be reduced. The reduction of emissions can lead to its own cost savings in that the production facilities might be sited in areas closer to the paving projects, thus reducing the haul distances, delivery time and associated costs.[13]

Whole asphalt cement is a thermoplastic material and therefore the viscosity is directly dependent on the material's temperature. At high temperatures asphalt cement softens and is more apt to flow, while at low temperatures the asphalt cement hardens becomes more brittle. Through a reduction of asphalt cement viscosity the material can be worked with at lower temperatures.[13] Also, with reduced asphalt cement viscosity the HMA aggregates are still effectively coated without experiencing the high rate of oxidation in higher temperature processes. This reduction of material viscosity is the key to WMA technology. There are currently four processes by which WMA material used in the United States is produced:[13, 14-17]

1) Hydrothermally crystallized synthetic zeolite (sodium aluminum silicate), when added to asphalt cement at temperatures of 85 ^{o}C or greater, will release a fine spray water molecules to the asphalt cement in which it is mixed. The release of the water droplets then creates foam within the asphalt cement which causes a volume expansion and reduces the asphalt cement viscosity. There are two commercial hydrothermally crystallized synthetic zeolite products currently on the market: Aspha-min® (Eurovia Services GmbH, Bottrop, Germany) and Advera® (PQ Corporation, Malvern, PA). The manufacturers recommend that these products be added to asphalt cement at 0.25 – 0.3 % by mass of the asphalt cement. These zeolite products are fully miscible with reclaimed asphalt paving, polymer modified and unmodified recycled asphalt cements. Zeolites are silicate framework structures with many void spaces. These voids are largely interconnected

and form channels throughout the crystalline matrix. It is within these channels that that water molecules can be trapped and firmly held within the zeolite crystalline structure through ionic interactions. Water held within these zeolite crystals is reported to be 21 % by weight. Heating to temperatures of 85 ^{o}C or greater causes the expulsion of the water molecules and produces the WAM material. Releasing the water does not destroy the zeolite crystalline framework structure.

2) WAM-foam® was developed through a joint venture between Shell International Petroleum Company, London UK and Kolo-Veidekke, Oslo, Norway. This technology involves separation of the asphalt cement into soft and hard components in a proprietary process. The two components are then added to the aggregate in separate production stages. The first stage involves mixing the soft asphalt cement component with the aggregate at approximately 110 ^{o}C until complete and intimate coverage has been achieved. The hard asphalt cement component is then introduced to the first stage mixture along with injection of cold water, producing a rapid volume expansion within the hard asphalt cement component and achieving the reduction in overall product viscosity. Care mast be taken in selecting the soft and hard asphalt cement components for production of a high-quality final product and thus may make this product incompatible with as wide of a range of asphalt cements as the other WMA technologies.
3) Evotherm™ (MeadWestvaco Asphalt Innovations, Charleston, SC)) utilizes emulsified asphalt cement combined with non-proprietary chemical additive packages to achieve an approximately 38 % reduction in production temperature. MeadWestvaco reports that the chemical additive package is

customized to be uniquely compatible with the specific aggregate used to construct the paving project.

4) Additives such as Sasobit® wax (Sasol Wax, South Africa), which has a melting point of 85 – 115 °C. Sasobit® wax differs from the naturally occurring bituminous waxes in that the average carbon chain length of naturally occurring bituminous waxes is on the order of 19 – 45 carbon chain length compared to an average carbon chain length of 40 – 115 carbons for Sasobit wax. The longer carbon chain length found in Sasobit wax results in a higher melting point than many naturally occurring bituminous waxes. Sasobit wax has been reported to be fully miscible with polymer modified, unmodified and recycled asphalt cements. When combined with asphalt cement at temperatures above Sasobit wax melting point, the wax liquefies and greatly lowers the overall HMA viscosity, reducing production and placement temperature by up to 50 °C.

The first two foam-related technologies along with Evotherm™ require extensive production equipment, making these studies beyond the scope of the current investigation. Material handling equipment for safe Sasobit composite production is available within our laboratory facilities. For this reason Sasobit has been chosen as one of the asphalt cement additives investigated in this study.

1.2. Sasobit®

Sasobit® wax is a paraffinic, brittle and highly crystalline hydrocarbon wax.[16] Sasobit wax is manufactured by the Fischer-Tropsch process from hydrogen and carbon monoxide through an iron (or cobalt) catalyzed, high-pressure reaction at 150-300 °C. Using the Fischer-Tropsch process, Sasol Corp. can maintain control over chain length, avoid branching and produce a wax free from contaminants (such as sulfur) often found in natural hydrocarbon sources. It is believed that the absence of double bonds along

the molecular chain backbone will alleviate oxidative chain scission in Sasobit wax and give long in-service life for this additive in asphalt pavings.

Sasobit wax is marketed by Sasol Corporation as a flow improvement and a low temperature deformation resistance additive.[17] The reduced mixture viscosity also improves compaction, as the placed HMA is less stiff with inclusion of Sasobit wax. Sasol Corporation reports that adding Sasobit wax at a 3 % loading on the total asphalt cement mass can also significantly improve deformation resistance in the Hamburg Wheel tracking test performed at 50 ^{o}C.

Kanitpong et al. investigated a 3 % loading of Sasobit wax (referred to as LCAH in the figures 1 – 3) in both AC 60/70 and a 5 % styrene – butadiene – styrene (SBS) polymer-modified asphalt cement of unknown PG grade along with control samples of each asphalt cement containing no Sasobit.[18] Their goal was to evaluate the energy required to achieve two different levels of mixture densification. They found remarkably improved performance from the Sasobit samples compared to the control samples. The most improvement came in the form of reduced energy expenditure to achieve the required compaction for opening the paving to general traffic flow.

The Maine(USA) Department of Transportation (MDOT) evaluated lab mixtures in 100 % reclaimed asphalt paving (RAP) prepared with two types of PG 64-28 (an emulsion asphalt cement of PG 64-28 base grade and a neat asphalt cement).[22] Sasobit formulations in 75% RAP were also conducted in a more robust laboratory mixture investigation by the same research group. Each investigation reported an average of 25 ^{o}C decrease in compaction temperature to achieve comparable densification as control samples along with a marked improvement in workability of the Sasobit loaded samples.

Edwards et al. have published literature on the rheological effects of Sasobit wax / asphalt cement mixtures on low and medium temperature performance.[24] They reported that at low temperatures, Sasobit modified asphalt cement increased in

complex modulus as measured through dynamic mechanical analysis (DMA) and increased stiffness under bending beam rheometer (BBR) creep testing. At medium temperatures, dynamic creep testing indicated an improvement in rut resistance in some of the Sasobit wax / asphalt cement samples tested.[25]

Sasobit wax has a high heat of fusion, and when mixed with a compatible polymer can become a phase change material (PCM).[26] Sasobit wax, as a PCM, can readily release energy to or store energy from the polymeric surroundings through melting or crystallization. When mixed with low density polyethylene (LDPE), Sasobit wax co-crystallizes with the polymer on cooling. The mixture of Sasobit wax / LDPE has been shown to reinforce the system in solid state at up to 50 % wax loading and was shown to reduce impact of both thermal and dynamic stress.

1.3. Elvaloy AM®

Elvaloy AM® (E. I. DuPont Nemours and Co.) is described as a reactive elastic terpolymer which binds with the asphalt to give excellent asphalt mixture reinforcement.[27] The term terpolymer refers to three different monomers comprising the polymeric chain. The monomeric units in this product are ethylene, butyl acrylate and glycidyl methacrylate (Figure 1.1). Glycidyl methacrylate has epoxide functionality and will readily react with thiyl, hydroxyl, amine or carboxylic acid functionalities on the asphaltenes to form a covalent bond of considerable strength. The ethylene (hard) and butyl acrylate (soft) monomers are used to adjust the glass transition of the polymer. Polacco et al. have reported the monomer composition as 66.7% ethylene, 28% butyl acrylate and 5.3% glycidyl methacrylate by mass.[28]

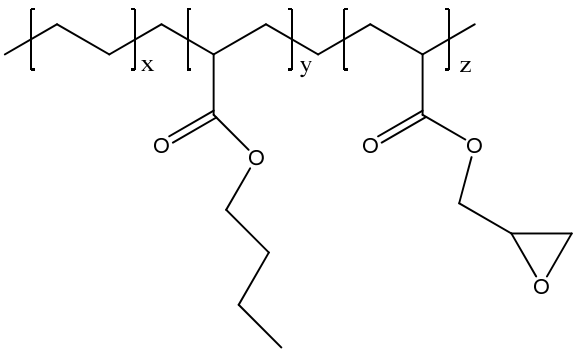

Figure 1.1 The polymeric structure of Elvaloy AM[28]

Currently the two most popular asphalt modification additives are styrene-butadiene-styrene (SBS) and crumb rubber.[29] Each of these materials has been shown to increase elastic recovery in the pavement which fades with oxidation. The double-bonds along these polymer backbones make them both vulnerable to oxidation. Both modifiers have also been shown to phase separate (when not crosslinked with sulfur during mixing with the asphalt in the case of SBS) from the asphalt paving over time resulting in reduced service life of that pavement. Elvaloy AM has the epoxide functionality through which it will form a covalently bonded network with the asphaltenes throughout the pavement making phase separation much less likely. The high rigidity of pavements modified with Elvaloy AM makes this an excellent additive for airport runway pavements and other high performance paving applications. Elvaloy Am's polymer backbone consists of sigma bonded monomer units and thus is not vulnerable to oxidative chain scission on the backbone chain.

Polacco et al. investigated the rheological aspects of Elvaloy AM modified asphalts and reported that there were two likely scenario's for this polymer's reinforcement of the colloidal system.[28] Bonding of the Elvaloy AM to the asphaltenes is primarily occurring within the pavement matrix. The polymer chain can also bond to

itself through cross-linking at the epoxide rings. The authors report that the inter-chain crosslinking reaction can be promoted though heat, a catalyst (polyphosphoric acid) or water molecules opening the epoxide ring and forming ester linkages with asphaltenes and ring-opened functional sites on the polymer backbone. This would result in a very robustly bonded system matrix and could easily result in an insoluble asphalt gel at too high a polymer load. The study warns that each composite of Elvaloy AM / asphalt cement should be carefully studied in terms of performance enhancement vs. gelation of the pavement.

Bhurke et al. investigated Elvaloy AM modification of an AC-5 asphalt cement HMA's through environmental scanning electron microscopy (ESEM) and low temperature fracture methods.[30] They found that at a loading of 2% Elvaloy AM (by weight of asphalt cement), the system achieved much greater stiffness compared to a range of styrenic co- and terpolymeric asphalt performance additives. The authors reported that the cured 2% Elvaloy AM modified binders exhibited comparatively reduced viscoelastic behavior and the fractures occurred with low fibril density. Cohesive failure (failure within the binder) was not observed and fracture was reported predominantly at the binder-aggregate interface.

In 2007, Khattak et al. also investigated Elvaloy AM in low temperature fracture and imaged the results of lap shear tensile tests with ESEM.[31] They also report that Elvaloy AM modified HMA's attained high stiffness and fracture resulted in course fracture faces exhibiting moderate fibrils. They also report that polymer concentration was not significant in terms of imaged effects on fracture morphology; with low Elvaloy AM loadings indifferentiable from higher loading results. A 2% loading on the asphalt cement was sufficient to achieve performance enhancement of laboratory HMA samples.

CHAPTER 2

EXPERIMENTAL

2.1 Raw Materials and Lab Aging of Materials

The asphalt cement used in all composite mixtures was PG 64-22 (Marathon Oil Corp). The Sasobit® wax (Sasol Corp.) was used as delivered in pelletized form. The loadings of Sasobit wax / asphalt cement ranged from 0.2-20 % by weight. Elvaloy AM® (DuPont Chemical Co.) was also used as delivered in pelletized form. Only one loading of 2 % Elvaloy AM / asphalt cement by weight was produced for this study to date. Short term aging of asphalt cement composites was performed with thin film oven aging (TFOT) as described in ASTM D1754.[32] Longer term aging of asphalt cement composites was performed using pressure aging vessel (PAV) as described in ASTM D6521.[33] ASTM specifications require that asphalt cement material be TFOT aged prior to PAV aging. PAV aging is performed to simulate the oxidation the asphalt cement should encounter through 5-10 years in-service

Physical mixing of the composites was performed in a two-piece glass kettle using a ¼ hp stir-motor and banana-blade stirring rod. A water-cooled condenser was attached to the kettle to maintain all composite vapors within the kettle during mix. A blanket of N_2 gas was maintained to avoid oxidation of the composite during mixing. A sample temperature of 100 ^oC was carefully maintained using a thermally monitored heating mantle for a 5 hr. sample mix time. Once mixed, the composite samples were transferred from the kettle to tightly capped aluminum “ointment canisters” for room temperature storage.

2.2 Differential Scanning Calorimetry

DSC experiments were performed on a TA 2920 MDSC instrument. Instrument control was provided through TA Instruments’ Thermal Advantage software and

thermogram analysis was enabled through TA Instruments' Universal Analysis software (TA instruments, New Castle, DE). Samples of the asphalt composites of 3 - 8 mg were weighed into covered and crimp-sealed aluminum pans. The method employed for DSC experiments unless otherwise specified:

1) temperature ramp of 10.00 ^{o}C/min to 150 ^{o}C
2) isothermal for 1.00 minute
3) temperature ramp of 1.00 ^{o}C/min to 25 ^{o}C
4) isothermal for 20.00 minutes
5) temperature ramp of 10.00 ^{o}C/min to 150 ^{o}C
6) end of method.

2.3 X-ray Diffraction

A Siemens-Bruker D5000 x-ray Diffractometer (Cu k_{α} radiation) was used for all X-ray analysis in this study. The tube voltage and tube current were 40 kV and 30mA, detector voltage was 840V. Experiments were run at ambient temperature (~22 ^{o}C) utilizing a step size of 0.02^{o} 2θ $s^{-1}$and a count time of 1 s / step, over a range of 2-70^{o} 2θ. The instrument was set-up with a divergence slit of 0.996^{o} prior to the sample and an antiscatter slit of 0.501^{o} (mounted between the sample and detector). A Kevex Psi peltier - cooled silicon detector with a 0.1 mm receiving slit was used to collect the raw data. The experiments were controlled through the use of Defract AT® version 3.1 operating software and the X-ray pattern processing was performed using a Jade® version 6.1 software package. The instrument calibration was performed using a Novaculite quartz standard (main diffraction of 2θ = 26.610^{o}). The collected data was normalized to a common baseline to aid in comparison of spectra features.

All X-ray diffraction samples were prepared in aluminum sample holders, having test specimen dimensions of 25 mm diameter and 2 mm thickness. Each sample was placed in an aluminum sample holder that was securely clamped to a piece of rigid ¼ inch Teflon sheet and placed in a 150 ^{o}C oven. After 10 minutes the molten sample was removed from the oven and a 1 mm thick, 27 mm diameter glass retaining slide was

mounted on the holder followed by a steel retaining clip to maintain the sample in the holder during testing (Figure 2.1).

Figure 2.1 The X-ray diffraction sample holder and fabrication pieces

2.4 Microscopy

Microscopy slide samples were produced by placing a small amount of Sasobit wax / asphalt cement composite on a clean glass side, then gently heating and melting the asphalt composite. The heating of the slide took place on a clean piece of aluminum foil covering a laboratory heating plate. A cover slide was then carefully placed over the molten asphalt composite sample. The cover slide was then steadily pressed with a clean wooden dowel rod until the molten sample appeared to be flat. Care was taken not to burn the composite sample while melting.

Elvaloy AM / asphalt cement Microscopy slides were produced by placing a small amount of the composite on a clean glass cover-slide, then gently heating and melting the asphalt composite. The heating of the slide took place as previously described using a laboratory heating plate. A glass slide was then carefully placed over the molten

asphalt composite sample. The slide was then loaded with a 200 g brass weight to achieve a more consistently flat sample profile along the interface of the cover-slide and asphalt composite sample.

The epifluorescence images were collected using a Leica DM RXA compound microscope equipped with a 20x 0.7 NA objective. The Cyan GFP filter set from Chroma Technology (31044v2) was chosen for all captured slide images. This filter-set has a 436/20 excitation filter and a 480/40 emission filter. A 455 nm dichromatic mirror produced the brightest images of the fluorescence from the imaged asphalt composite samples. Images were collected using a Sensicam QE (Cooke Corp) 12-bit, cooled CCD camera and a 100 ms exposure time for each image. Slidebook® (Intellegent Imaging Innovations) software was used to process the collected images. For the Sasobit / asphalt cement samples, a "no-neighbors" deconvolution (simple de-blurring) algorithm was used to reduce background light and sharpen contrast. For the Elvaloy/ asphalt cement samples, the deconvolution algorithm was not employed in the treatment of the images prior to presentation.

The scanning laser confocal microscopy images were acquired using a Leica TCS SP2 scanning laser confocal microscope equipped with a 20x 0.7NA objective. The images in this work were obtained by collecting sequential images at different focal planes through the upper 5 microns of the sample using a 488 nm laser to illuminate the sample and collecting light between 512 and 553 nm to produce each individual image. The data from these images were combined using an average projection to form a single image. The images were pseudo-colored to make the features of interest more apparent.

2.5 Gel Permeation Chromatography

A Polymer Laboratories model PL-210GPC (Shropshire, UK) was used for analysis of all GPC samples. In addition to the standard differential refractive index (dRI) detector used for concentration detection, two molecular weight sensitive detectors

are installed in the PL-210GPC; a Precision Detectors (Bellingham, MA) model PD-2040 dual angle laser light scattering (LS) detector and Viscotek (Houston, TX) model 210 Differential Viscometer (DV). The detectors are installed in series configuration with the LS being first after the chromatographic columns, followed by the dRI and lastly the DV.

The mobile phase was 1, 2, 4-trichlorobenzene (TCB) stabilized with approximately 125 ppm of 3, 5-di-*tert*-butyl-4-hydroxytoluene (BHT). The mobile phase flow rate was 1.0 mL/minute. The TCB was recovered from a B/R Instruments distillation unit. The TCB was filtered through a 0.020 μ filter before adding the BHT, and once on the instrument was purged continuously with a slow bubbling of nitrogen. The mobile phase was further degassed by flowing through a vacuum degasser before entering the pump of the PL-210GPC.

The Polymer Laboratories PLgel® column set consists of three analytical columns and a guard column. Each analytical column measured 300 mm in length with an inside diameter of 7.5 mm. The guard column was 50 mm by 7.5 mm. The column set was mounted in the oven compartment of the PL-210GPC. All experiments were performed at 145 °C.

The molecular weight sensitive detectors were calibrated by injecting a known mass of the PE53494-38-4 linear polyethylene standard (Mw = 115,000 Da, IV = 1.783 dL/g). Polystyrene standards manufactured and characterized by Polymer Laboratories were used for column calibration.

2.6 Rheology

All rheology experiments reported in this work were performed on an AR2000 controlled - stress dynamic shearing rheometer (TA instruments, New Castle, DE). This instrument was capable of reproducing torque values up to 200 mN*m. Thermal control during experiments was maintained using an environmental test chamber (ETC). This electrically heated, highly insulated ETC could be cooled either though compressed air

or with liquid nitrogen flowing through the ceramic manifold within the ETC housing. The AR 2000 instrument was capable of maintaining testing temperatures within the sample chamber to ±0.1 ^{o}C. TA Rheology Advantage software controlled instrumental settings. The DSR instrument utilized a very low friction air bearing driven by 30 psi compressed air. The geometry selected for frequency sweep experiments performed in this work was stainless steel 8 mm diameter parallel plates.

Prior to test specimen fabrication, asphalt cement samples were heated in a 150 ^{o}C laboratory for approximately 15 minutes. The molten asphalt cement or composite was poured into silicone rubber molds to form the test specimen. Each test specimen was allowed to solidify at room temperature undisturbed for 20 -30 minutes prior to mounting between the parallel plates. A precisely maintained sample gap of 2 mm was used with the 8 mm plate geometry for each experiment.

The frequency sweep experiment was a controlled strain and continuous oscillation procedure. Temperature steps of 30, 40, 50, 60 and 80 ^{o}C and an oscillation frequency range of 0.01 – 25 Hz (3 testing frequencies per decade) per step. A 30 min thermal equilibration at each temperature step was programmed for each experiment. A 10 second sample relaxation time between frequency changes was utilized along with a 1 % shearing strain value for all experiments.

CHAPTER 3

RESEARCH PROGRESS DISCUSSION

3.1. Gel Permeation Chromatography

Normally the Daly and Negulescu research group has performed Gel Permeation Chromatography (GPC) experiments at room temperature using tetrahydrofuran (THF) as both the sample solvent and elution solvent. THF is not a solvent that paraffinic Sasobit nor the Elvaloy AM terpolymer will dissolve in. Therefore, all of the GPC samples in this experiment were dissolved in and eluted using trichlorobenzene (TCB).

All of the samples were eluded through a dual angle laser light scattering (LS) detector, refractive index (RI) detector and differential viscometer (DV) detector connected in series. The quality of each data set collected for the set of samples was not consistent. For example, the neat Sasobit and Elvaloy samples were sufficiently clear solutions when solvated in TCB to allow for LS data analysis. On the contrary, the asphalt cement and additive composite samples were darkly colored solutions and the LS detector could not collect high-quality data from these samples. The data sets collected from the DV detector across the sample set tended to be noisy. Also, the baselines for each DV detector dataset were not the same due to fact that the initial concentrations of each sample were not exactly the same. The data sets collected from the RI detector were of acceptable quality and low noise but the value of differential concentration (dn/dc) for both Sasobit and Elvaloy AM read negative with respect to the asphalt cement dn/dc in TCB. Taking these facts into consideration, a decision was made to analyze the GPC-RI data for all of the samples investigated. Since the RI detector collects data in terms of dn/dc this seemed to be the most appropriate data to compare across the entire sample set.

Three of the most common methods of evaluating the molecular weight averages for a sample are M_n, M_w and M_z.[34] M_n represents the number average molecular weight or the total weight of all polymer chains within a sample divided by the number of molecules within that sample. The number average molecular weight is considered to be more accurate for a low-molecular weight sample. M_w is referred to as the weight-average molecular weight. In higher molecular weight average samples the higher molecular weight components contribute more to the total sample molecular mass then the low-molecular weight components. Therefore for higher molecular weight samples M_w is considered to be a more accurate way to report the molecular weight average information. M_z is referred to as the z-average molecular weight and it encompasses more of the area bound by the GPC molecular weight curve. These molecular weight averages are graphically presented in a typical molecular weight distribution curve (Figure 3.1).[35]

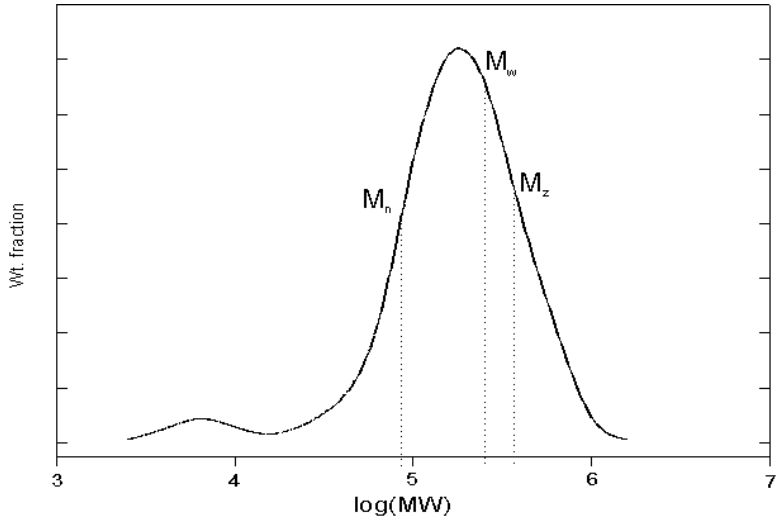

Figure 3.1 A typical molecular weight distribution GPC curve [35]

Of the three molecular weight averages, the most often reported are M_n and M_w. The polydispersity index (PDI) or M_w/M_n, represents a standard method to express the breadth of the molecular weight distribution within the sample. The value of M_n, M_w and M_z can be calculated as follows:

$$M_n = \frac{\Sigma(N_i M_i)}{\Sigma N_i} \qquad M_w = \frac{\Sigma(N_i M_i^2)}{\Sigma(N_i M_i)} \qquad M_z = \frac{\Sigma(N_i M_i^3)}{\Sigma(N_i M_i^2)}$$

These molecular weight averages and PDI are only reported for the neat Sasobit and Elvaloy samples as these respective chromatograms exhibit one continuous GPC curve without distinctly separated peaks. In the asphalt cement and the additive composite chromatograms we have more than one distribution of molecular weight components; therefore, it is more convenient to comment upon molecular weights at particular points along the respective GPC curves in effort to show how the overall system is changing.

In the GPC-RI curve for the neat Sasobit sample (Figure 3.2) the value of PDI was determined as 1.33. Theoretically, a mono-disperse GPC sample would have a PDI of 1.0 with the values of M_n and M_w being equal. This rarely happens in many synthetic polymers with exception of some polymer standard samples. The value of M_n, M_w and M_z for the neat Sasobit GPC-RI sample has been determined as 750, 1000 and 1400 Daltons respectively (Figure 3.2). The values for the peak molecular mass has been indicated in Figure 3.1.2 as 1.65K Daltons.

The GPC-RI curve for the neat Elvaloy sample (Figure 3.3) shows that this sample has a PDI of 4.61. The neat Elvaloy PDI of this magnitude compared to the neat Sasobit PDI indicates the neat Elvaloy sample has a greater range of molecular weight components. Also, the average molecular mass of the high molecular weight components is greater in the neat Elvaloy sample than in the neat Sasobit sample. The

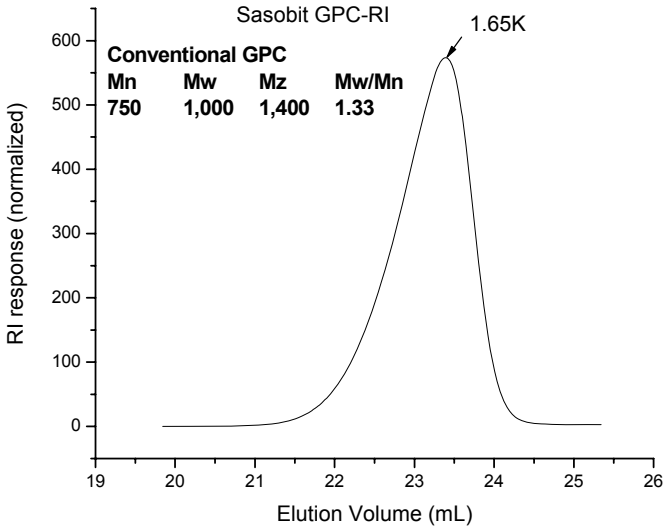

Figure 3.2 The GPC-RI chromatogram for neat Sasobit

value of M_n, M_w and M_z for the neat Elvaloy GPC-RI sample has been determined as 18,080, 83,380 and 288,300 Daltons respectively (Figure 3.3). The values for the peak molecular mass and the high molecular weight shoulder are indicated in Figure 3.3 as 72K and 805K Daltons respectively.

In the GPC-RI chromatogram for neat PG64-22 (Figure 3.4) we see that there are clearly two peaks and the higher molecular average mass peak exhibits a shoulder. The shoulder area is designated by an approximate molecular mass of 6.4K Daltons with an arrow pointing out the approximate apex. The shoulder is believed to be an indication of asphaltene aggregation and appears most prominent in the PG 64-22 PAV curve. The shoulder appears in the PG 64-22 Original curve but not as prominent as in the PG 64-22 TFOT or PG 64-22 PAV curves. In general, as the sample ages the asphaltene aggregates achieve approximately 6.4K Daltons and increase in concentration through laboratory sample aging. The values for the low molecular mass peak (believed to be the maltene fraction) across this particular sample set all exhibit the

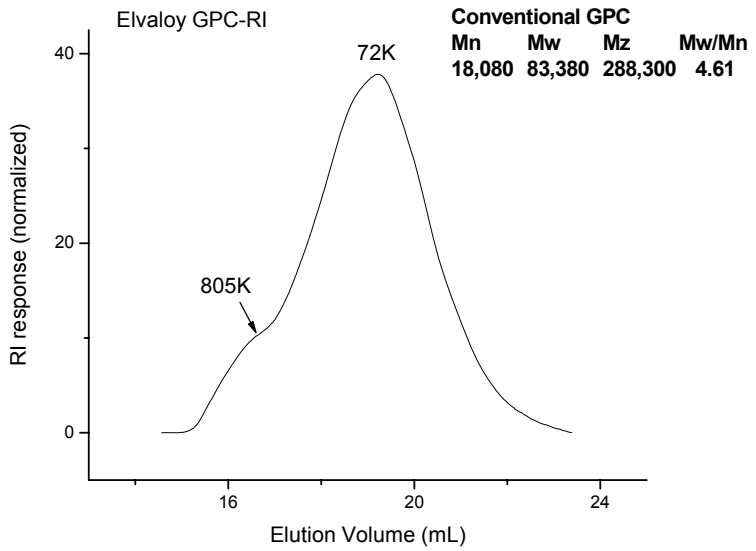

Figure 3.3. The GPC-RI chromatogram for neat Elvaloy

same molecular mass of approximately 543 Daltons for each peak molecular mass value, although the relative maltene concentration decreases on aging. On the higher molecular mass peak (believed to be the non-aggregated asphalt fraction), we see that peak value increases only slightly with each laboratory sample aging step. This sample set can be considered the control set in terms of the additive composite sample aging studies.

In the GPC-RI chromatogram for 1% Sasobit / PG64-22 composites (Figure 3.5) we again see that there are clearly two peaks and a higher molecular average mass peak exhibiting a shoulder. In general, as the sample ages from original through PAV, the asphaltene aggregate shoulders achieve approximately 6.8, 6.7 and 6.1K Daltons but don't clearly show a marked increase in concentration through laboratory aging until the PAV aging step. Realizing that the dn/dc value of the Sasobit reads negative with respect to the asphalt cement, the true molecular mass values for this shoulder should show higher magnitude. I believe that as the 1% Sasobit / PG64-22

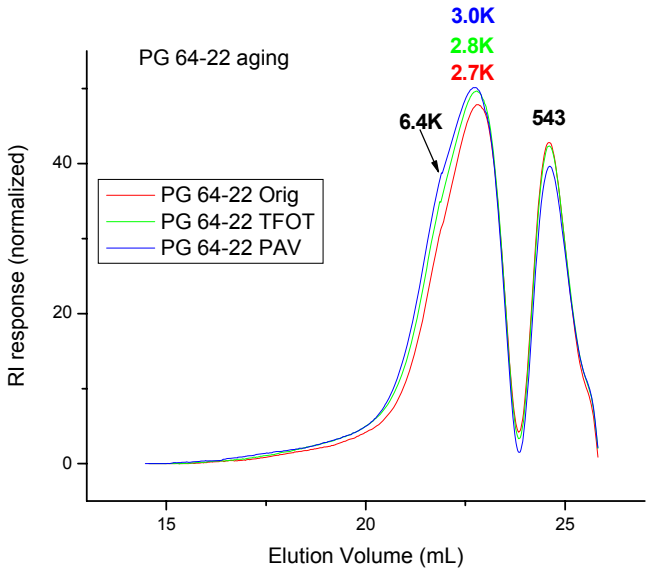

Figure 3.4 The GPC-RI chromatogram overlay for neat PG64-22 sample laboratory aging

composites are aged through these laboratory methods with temperatures exceeding the melting point of the additive, the Sasobit goes into solution. Upon cooling of the sample and allowing the wax to re-crystallize, it may be that the Sasobit wax could preferentially crystallize on the aliphatic side chains of the asphaltene molecules. This should lead to a higher molecular mass value for the shoulder on sample aging and also increase the asphaltene aggregate concentration. The values for the peak believed to be the maltene fraction across the Original and TFOT chromatograms exhibit the same molecular mass of approximately 554 Daltons for each peak molecular mass value. The peak molecular weight value for the PAV sample decreases to approximately 542 Daltons. This may indicate that some of the Sasobit wax may crystallize with the lower molecular weight component of the maltene fraction and that following PAV aging a percentage of the Sasobit component crystallizes on the aliphatic side chains of the non-aggregated asphaltene and asphaltene aggregate molecules. On the non-aggregated asphaltene

fraction peaks, we see that peak value again increases by approximately 100 Daltons with each laboratory sample aging step. This may indicate that due to the lower viscosity in the molten Sasobit composite samples during both aging steps, the asphaltene molecules achieve more mobility and are therefore more likely to aggregate then in the control samples. In Figure 3.6 we clearly see that most of the neat Sasobit samples molecular mass envelops the non aggregating asphaltene peak and asphaltene aggregate shoulder along with a portion of the high molecular weight maltene fraction.

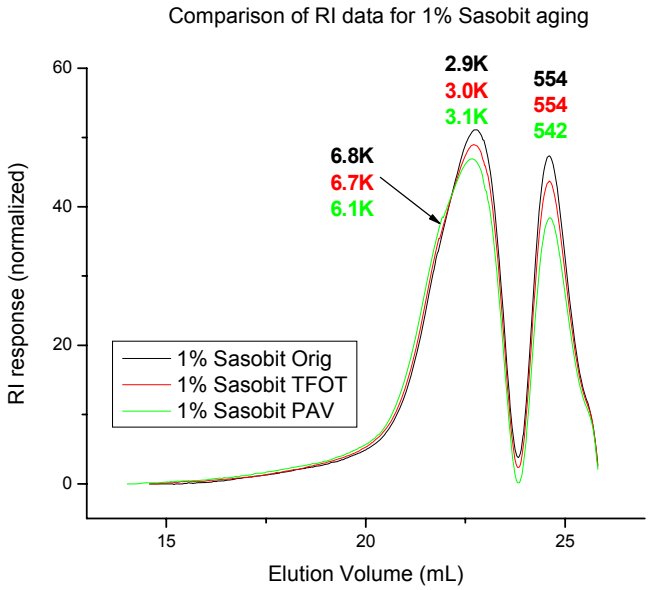

Figure 3.5 The GPC-RI chromatogram overlay for 1% Sasobit composite sample laboratory aging

In the GPC-RI chromatogram for 2% Elvaloy / PG64-22 composites (Figure 3.7) we see two separated peaks with the higher molecular average mass peak exhibiting a shoulder. In general, as the sample ages from original through PAV, the asphaltene aggregate shoulders achieve approximately 6.7K Daltons but show marked increase in concentration through laboratory aging at each step. Realizing that the dn/dc

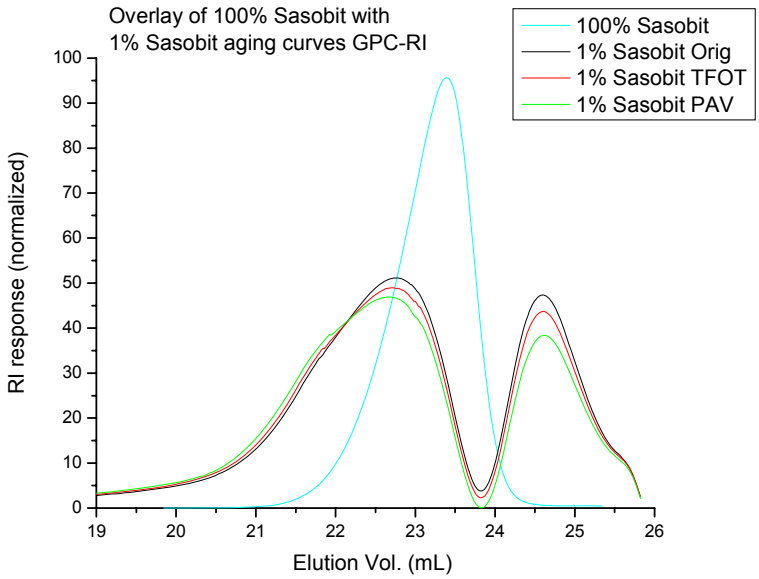

Figure 3.6 The GPC-RI chromatogram overlay for neat Sasobit and Sasobit composite samples laboratory aging (100 % Sasobit chromatogram re-scaled)

value of the Elvaloy reads negative with respect to the asphalt cement, the true molecular mass values for this shoulder should be greater. Polacco et al. have reported that Elvaloy will bond to the asphaltenes.[28] Through this bonding a sharp jump in molecular mass and concentration for the non aggregating asphaltene peak and asphaltene aggregate shoulder should be exhibited, but the reverse is exhibited. We see roughly that same trend as was exhibited in the control samples with respect to the maltene peak molecular mass fraction. The values for the peak believed to be the maltene fraction in the Original and TFOT chromatograms exhibit the same molecular mass of approximately 554 Daltons for each peak molecular mass value. As the Elvaloy composites are aged through current laboratory methods with temperatures high enough to initiate some of the epoxy functional groups to bond (Polacco et al. Reference 28) with the asphaltene fraction or itself, we may see the first stage of a covalent network gel forming within these composites. This should lead to a higher molecular mass value at

both the shoulder and the non - aggregating asphaltene peak aggregating asphaltene shoulder on sample aging if it is occurring. There is a marked increase in both the non aggregating asphaltene peak and the asphaltene aggregate shoulder concentrations. Referring to Figure 3.8 we clearly see that the lower molecular mass tail of the neat Elvaloy sample covers the non aggregating asphaltene peak and asphaltene aggregate shoulder and not much of the maltenes peak.

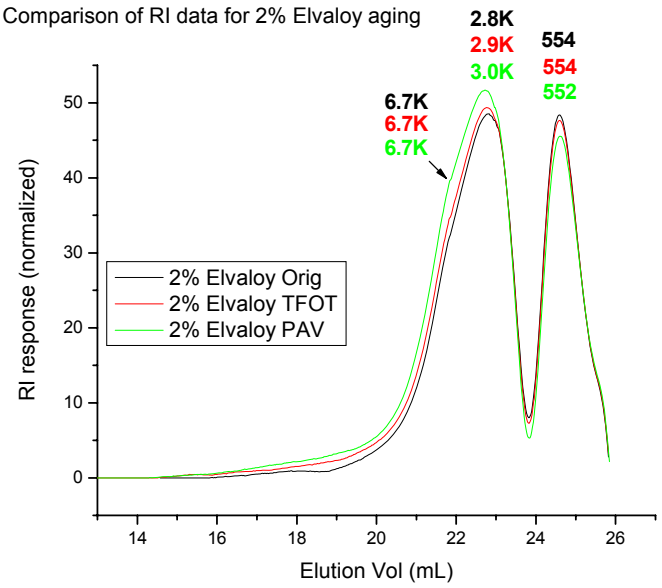

Figure 3.7 The GPC-RI chromatogram overlay for 2% Elvaloy composite sample laboratory aging

Upon review of the presented GPC-RI data an interesting anomaly has been noticed. It seems that the asphaltene component appears to make up the larger portion of the whole asphalt cement sample across the sample set. This may be due to the more polar make-up of the asphaltene fraction and its interaction with the solvent. TCB is a very polar solvent and therefore may be interacting more with the polar components of the samples. This would effect the true representation of the concentration distribution of asphalt cement components. Even with this consideration in mind, the

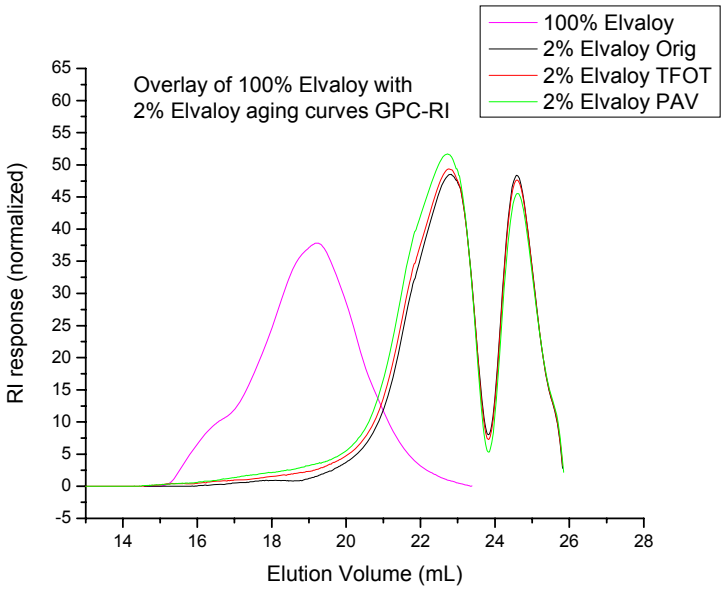

Figure 3.8 The GPC-RI chromatogram overlay for neat Elvaloy and Elvaloy composite samples laboratory aging

trends discussed are evident within the particular data sets and have given insight to molecular mass and concentration changes within the various components making up the samples analyzed.

3.2. Differential Scanning Calorimetry

One of the unique distinguishing features of the pure Sasobit wax is the existence of several overlapping endothermic transitions evidenced within the differential scanning calorimetric heating curves.[36] Alkane chains at low temperature have been reported to exist in a number of crystalline forms; triclinic, orthorhombic, monoclinic and hexagonal.[37, 38] Some alkanes have also been reported to have one or more rotator crystalline phase transitions exhibited between the crystalline and isotropic liquid state.[39, 40] In Figure 3.9, two differential scanning calorimetric heating curves are presented for comparison.[36] The upper curve is that of a soft paraffin wax (Wax S) from Slovnaft (Bratislava, Slovakia). The heating curve for Wax S exhibits two distinct thermal

transitions identified by the peak temperatures of 40.7 ^{o}C and 56.8 ^{o}C. Luyt and Krupa have determined that the 40.7 ^{o}C transition is associated with a solid-solid transition and suggest that this transition may be an orthorhombic to hexagonal crystalline phase transition. The authors report that the 56.8 ^{o}C transition represents a complete melting of the crystallites in a solid to liquid phase transition. The lower curve in figure 3.9 represents the heating curve for a Sasobit wax (Wax FT). The Wax FT curve exhibits a distinctly different thermal transition profile, with evidence of multiple overlapping endothermic transitions at 83.6 ^{o}C, 91.2 ^{o}C and 104.9 ^{o}C. Luyt and Krupa attribute this thermal behavior to the melting of different mass fractions within the neat wax.[36]

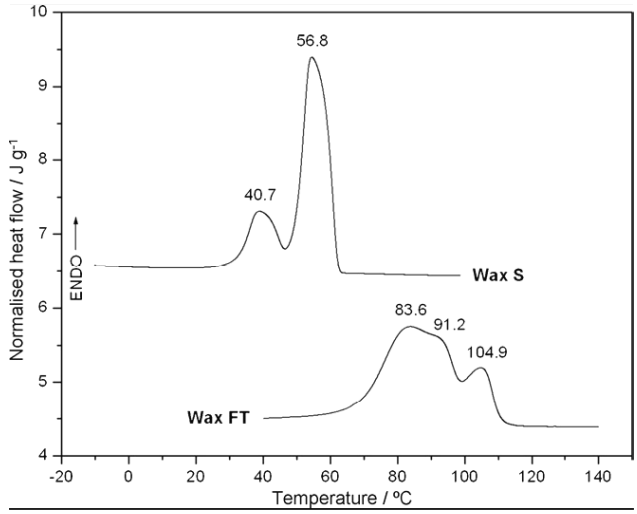

Figure 3.9 DSC heating curves of Wax S and Wax FT [36]

The highly crystalline structure of Sasobit wax allowed for DSC to be used in determination of the loading of this additive to the neat asphalt. As can be seen in the DSC cooling curves (figure 3.10), the lowest (magenta colored) curve belongs to the neat asphalt cement shows negligible crystallinity compared to the other samples over the temperature range presented. Loadings of Sasobit from 1 % in neat asphalt cement

to 100 % Sasobit wax show unique and distinctive crystalline phases within the samples with the onset peak temperature of crystallization increasing as the wax loading increases.

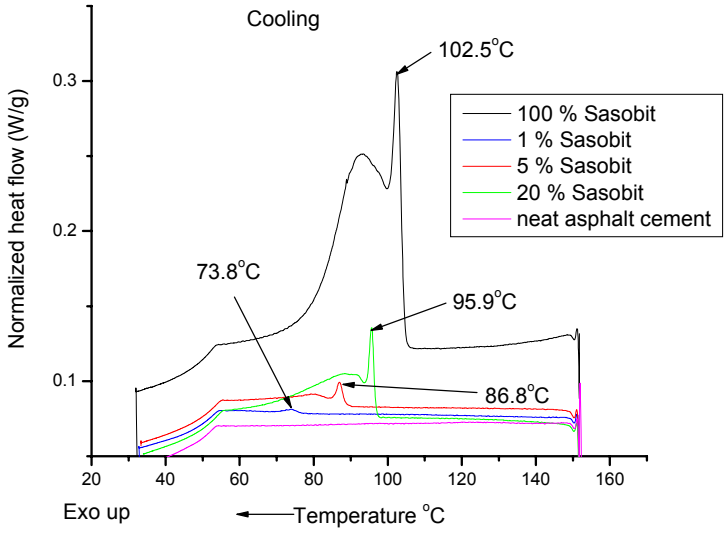

Figure 3.10 DSC cooling curves for a range of Sasobit loadings

From the heating curves (Figure 3.11) the blue colored 1% Sasobit trace indicates the additives presence in the mixture with the maxima occurring approximately 73.8 °C. With the increase in Sasobit load, we see a very distinctive shape of the curve indicating that there are multiple transitions occurring during both crystallization and melting.

Analysis of the DSC heating curve enthalpy (ΔH) data shows that there is less deviation from the expected ΔH values on the first heating than on the second heating (Table 3.1). The "expected ΔH value" is calculated through multiplying the ΔH value of the 100 % Sasobit (orange colored trace) sample by the Sasobit weight % / 100.00 in each composite sample. There appears to be no clear co-crystallization indication in the data

presented for the Sasobit / asphalt cement composites, as the difference between expected and measured ΔH values are not of significant magnitude.

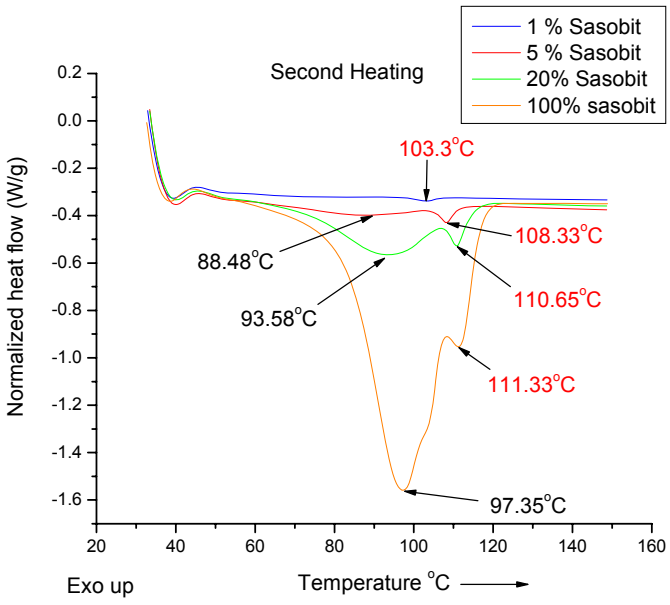

Figure 3.11 DSC heating curves for a range of Sasobit loadings

Table 3.1 DSC heating curves Enthalpy data for Sasobit composites

Mixture	Heating (1^{st},2^{nd}) ΔH (J/g)	Expected ΔH (J/g)	Difference (J/g)
100 % Sasobit	181.40, 170.10	181.40, 170.10	0.00
20 % Sasobit	36.82, 34.33	36.28, 34.02	0.54, 0.31
5 % Sasobit	9.01, 8.06	9.07, 8.51	-0.06,-0.45
1 % Sasobit	0.58, 0.42	1.81, 1.70	-1.23, -1.28

To explain the negative difference in the 1 % Sasobit ΔH values one must zoom in on the cooling section of the DSC curve for the neat asphalt used in formulating the composite samples (Figure 3.12). There can be clearly seen an exotherm indicating that the asphalt cement does indeed exhibit crystallization.

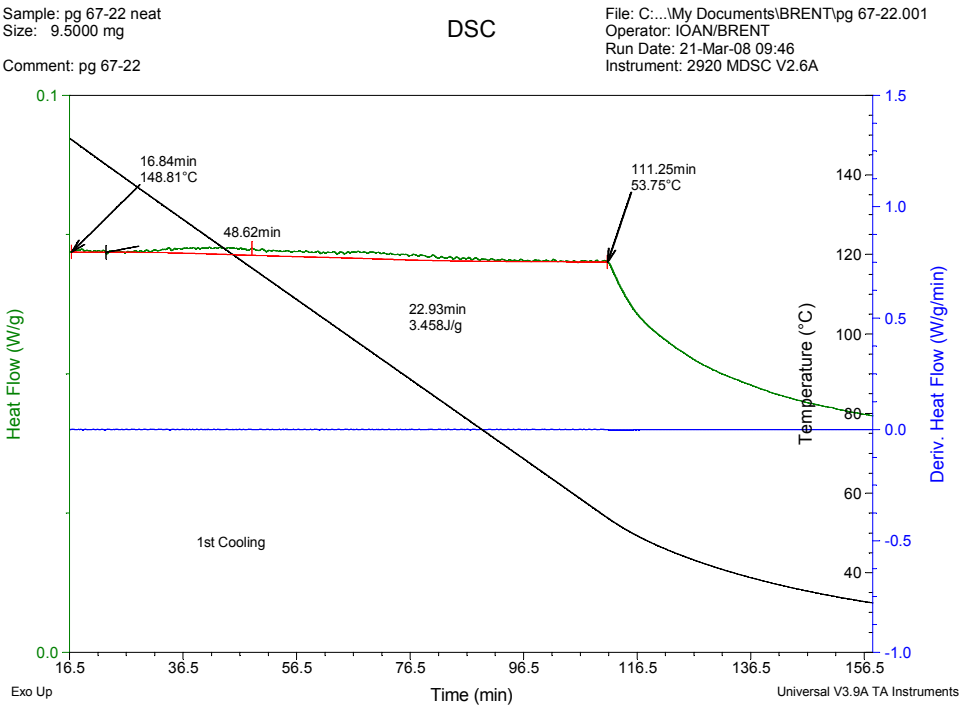

Figure 3.12 The DSC cooling curve for neat asphalt cement

Daly et al. have investigated eight asphalt cement samples ranging in grade from AC10 to AC30.[41] They have reported that with proper annealing of the asphalt cement sample, one can expect to reveal from one to four exothermic transitions over a range from approximately 0 ^{o}C to approximately 60 ^{o}C. They also have reported that in order to enhance the crystallinity of a particular fraction within the asphalt cement sample, one must anneal the sample at a temperature approximately 10 ^{o}C below the expected onset temperature of the expected endothermal transition.

Masson and Polomark reported that an endothermic transition centered at approximately 70 ^{o}C in the MDSC thermogram for an asphalt cement, could be attributed to the asphaltene fraction.[42] The authors also reported that ordering within the asphalt cement sample occurred in three stages and is time dependent. They reported that the first stage of ordering took place in the low molecular mass maltene phase and occurred rapidly as the molten asphalt cement cooled and quenched at 22 ^{o}C. A second stage in the ordering processes involved the medium molecular mass molecules in the maltene phase and completes in approximately 3 hrs. The third stage in ordering within asphalt cement involved the asphaltenes and the highest molecular mass molecules in the maltene phase. This stage was reported to last for 16 – 24 hrs resulting in a thoroughly annealed asphalt cement sample.

Due to the fact that asphalt cement must be properly annealed prior to thermal analysis using DSC, a new program was utilized in the present investigation:

1) ramp 10.00 °C/min to 150.00 °C
2) isothermal for 1.00 min
3) ramp 1.00 °C/min to 40.00 °C
4) isothermal for 720.00 min
5) ramp 1.00 °C/min to 25.00 °C
6) isothermal for 20.00 min
7) ramp 10.00 °C/min to 150.00 °C

As a result of this annealing program, the measured enthalpy on the second heating cycle for the 1% Sasobit / asphalt cement sample (figure 3.13) dramatically increased from 0.42 J/g to 2.042 J/g with 12 hr annealing at 40 ^{o}C. This suggests that at a loading of 1 % Sasobit / asphalt cement there may indeed be co-crystallization between Sasobit and the asphaltene fraction of the sample. It also suggests that the concentration of Sasobit in the 1% sample may be slightly greater than 1% in this composite. It is believed that the 5 % and 20 % Sasobit loadings may disrupt the asphaltene stacked crystalline structure model (Figure 3.16) to be introduced in the X-ray diffraction chapter

(Chapter 3.3) of this thesis leading to no contribution from the asphaltenes to these measured enthalpies.

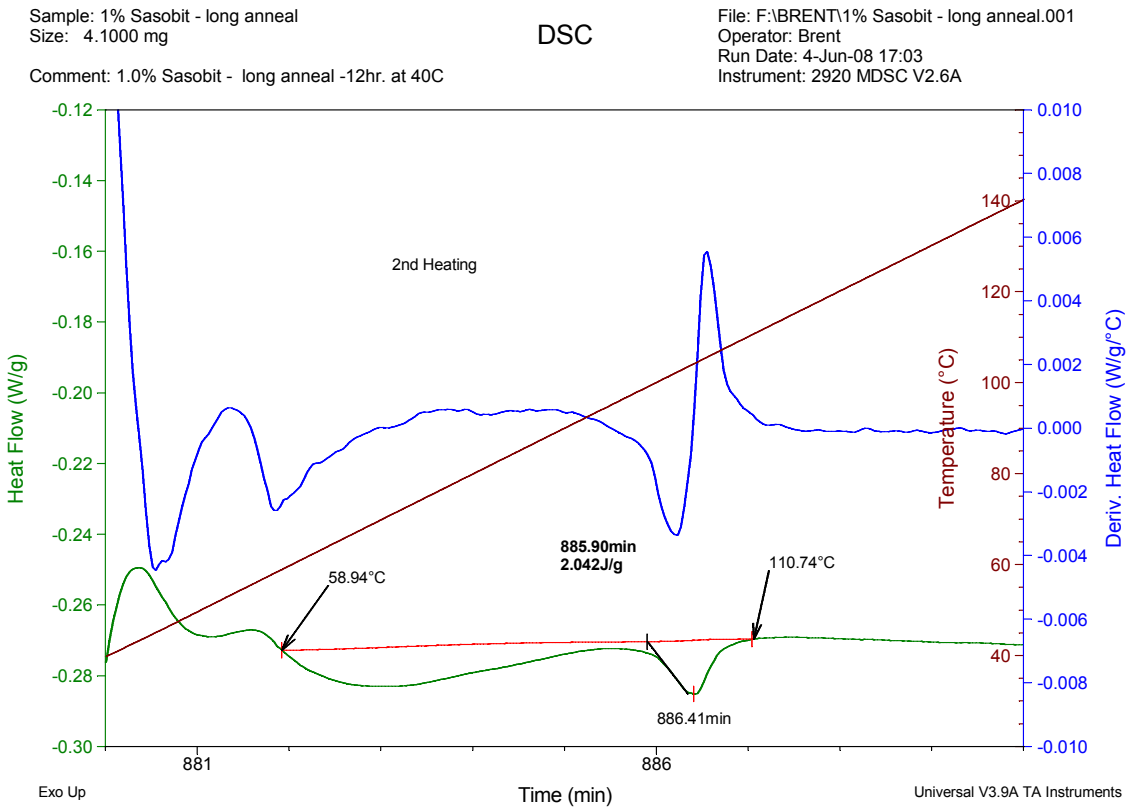

Figure 3.13 The DSC cooling curve for 1% Sasobit / asphalt cement

The 0.2 % Sasobit / asphalt cement sample second heating thermogram (Figure 3.14) explicitly shows two separate endothermal transitions. The lower temperature transition located between 53.02 ^{o}C and 77.64 ^{o}C (ΔH = 0.3209 J/g), can be attributed to the asphaltene fraction (Masson and Polomark Reference 42), while the transition located between 86.94 ^{o}C and 100.51 ^{o}C (ΔH = 0.07742 J/g) can be attributed to the Sasobit. This might indicate that a loading of Sasobit of this magnitude in asphalt

cement might not be significantly disrupting the stacked crystalline structure (Figure 3.16) of the asphaltenes and may be co-crystallized with the asphaltene fraction.

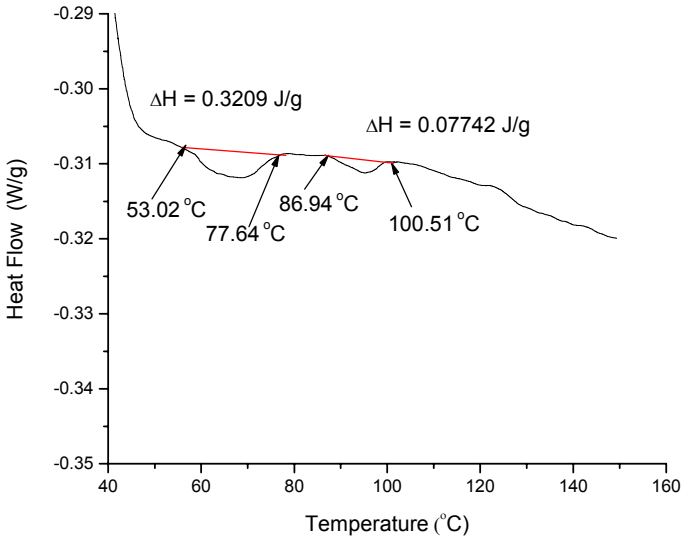

Figure 3.14 The DSC heating curve for 0.2% Sasobit / asphalt cement

When the PG 64-22 sample was annealed in the same manner as the 0.2 % Sasobit / asphalt cement, sample evidence of an endothermic transition located between 56.54 ^{o}C and 77.64 ^{o}C during the second heating was revealed (Figure 3.15) and likely could be attributed to the asphaltene component (Masson and Polomark Reference 42). Alternatively, the first transition (between 56.54 ^{o}C and 77.64 ^{o}C) could be Sasobit wax crystallized on the asphaltene side chains and the second transition (between 86.94 ^{o}C and 100.51 ^{o}C) could be homogeneous regions of Sasobit wax.

This possibly indicates that a low percent loading of Sasobit reduced the total enthalpy within this endothermic transition. This also might give an indication of why the enhanced performance loading range (0.8 % - 3 % on asphalt cement mass from References 16 and 17) of Sasobit in asphalt cement has been experimentally

determined. If Sasobit co-crystallizes with the asphaltene fraction to an extent that the asphaltene stacked crystalline structure (Figure 3.16) is somewhat preserved and a symbiotic relationship between the two may lead to enhanced system performance.

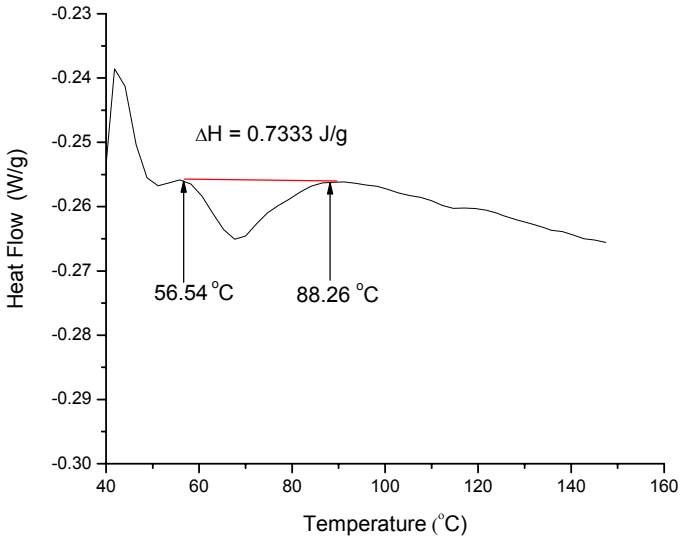

Figure 3.15 The DSC heating curve for PG64-22 asphalt cement

A second batch of Sasobit (Sasobit H8) was received and formulations of 6, 4 and 2% were produced in the same way as described in Chapter 2.3 of this work. The DSC method used in their analysis is the same as is presented in the experimental section of this paper. The second heating curve was integrated and is presented Table 3.2. The 4% and 6% Sasobit H8 composite sample enthalpies come very close to the calculated values but the enthalpy for the 2 % sample has a difference of -0.68 J/g with respect to the calculated enthalpy. This discrepancy may result from the concentration of Sasobit being slightly greater than 2% Sasobit in that sample due to an initial weighing error during the laboratory mixing stage but also may indicate co-crystallization that doesn't completely disrupt the London force attractions between asphaltene molecules.

Table 3.2 Analysis of the second heating curve for Sasobit H8 composites

Composite	2nd Heating ΔH (J/g)	Calculated ΔH (J/g) (ΔH 100%) * wt%	Difference
100% Sasobit H8	188.00	188.00	0.00
6% Sasobit H8	11.25	11.28	0.03
4% Sasobit H8	7.53	7.52	0.01
2% Sasobit H8	3.08	3.76	-0.68

3.3. X-ray Diffraction

A number of X-ray diffraction studies have investigated the powder diffraction pattern arising from asphaltenes chemically precipitated from asphalt cement in both Original and laboratory aged samples.[43-46] These investigators calculated the structural (aromaticity and crystallite) parameters found in the asphaltene powder samples to produce a cross-sectional model (Figure 3.16) using collected X-ray diffraction data.[43] As can be seen from the asphaltene cross-sectional model, the aromatic portions of the molecule tend to form stacks under the influence of London dispersion forces (also referred to as pi-stacking). Aliphatic side chains are represented within the asphaltene model extending from the central aromatic portion of the asphaltene molecule. These side chains are likely to be the template sites for wax crystallization. A characteristic asphaltene X-ray diffraction pattern and real diffraction data is shown in Figure 3.17 along with a representation of the reflection planes associated with each diffraction.[44, 45]

Lu and Redelius have isolated naturally occurring paraffin waxes from asphalt cement and investigated their X-ray diffraction spectra (Figure 3.18).[47] From these

studies it has been concluded that asphaltenes and waxes isolated from asphalt cement can crystallize within the asphalt cement.

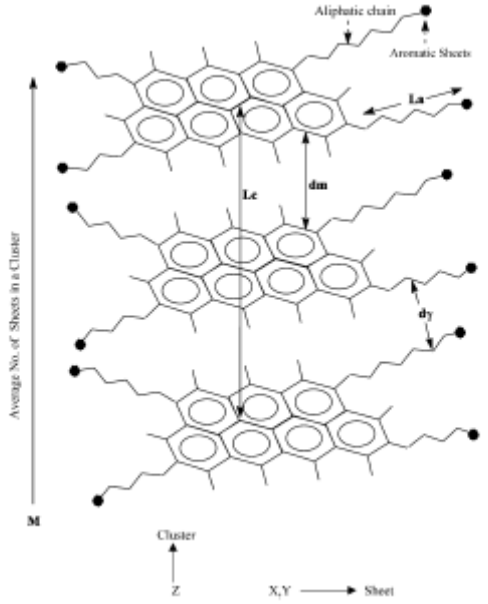

Figure 3.16 A Model of asphaltene molecules in the stacked crystalline form [45]

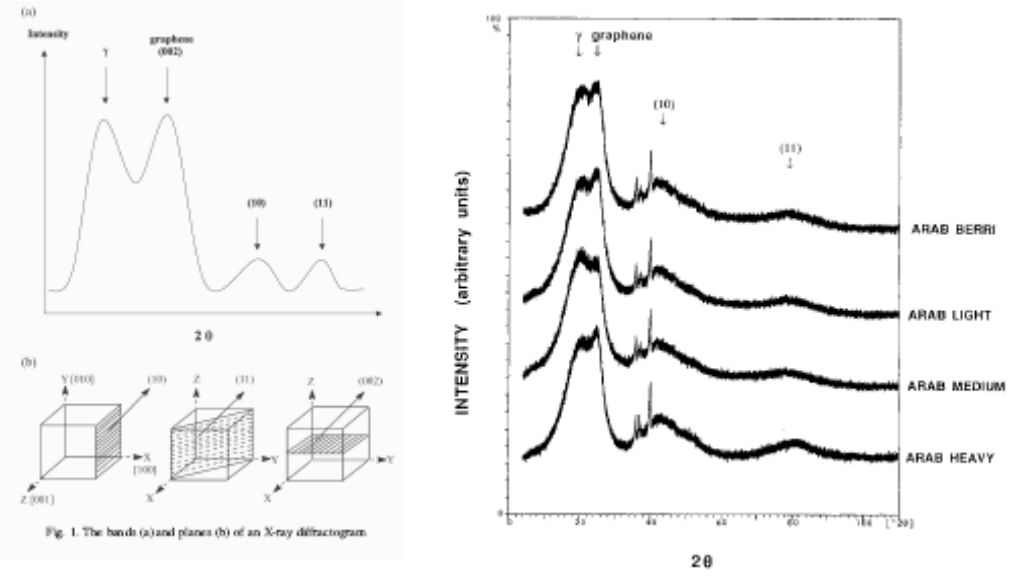

Figure 3.17 Representative precipitated asphaltene X-ray diffraction patterns[44, 45]

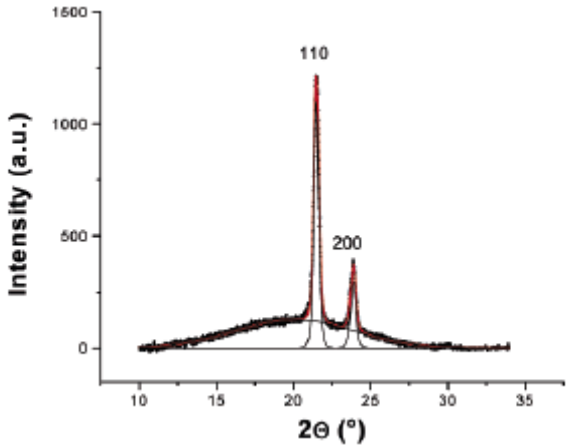

Figure 3.18 X-ray diffraction pattern for naturally occurring paraffin waxes isolated from asphalt cement [47]

The two main diffraction peaks arising from crystalline asphaltenes occurred at approximately 20° and 25° values of 2θ.[43] The two main diffraction peaks arising from crystalline waxes occur at approximately 21.2° and 23.4° values of 2θ with the assignment of X-ray reflection planes of (110) and (200) respectively.[47]

From the X-ray diffraction pattern overlays (Figure 3.19) the evidence for loadings down to 2 % Sasobit in asphalt cement can be easily discerned through the diffractions at 2θ = 21.2° and 23.4°. For the 1 % and 0.2 % Sasobit / asphalt cement samples the diffraction at 2θ = 21.2° is the only diffraction that can be clearly discerned. Therefore, this may indicate that either there was some interaction in the form of co-crystallization that doesn't separate the asphaltene molecules beyond their London force attraction range between the Sasobit and asphalt at these loadings or that the Sasobit species at these low concentrations crystallized (Chapter 3.2. DSC data) but the noise in the X-ray diffraction pattern overwhelmed the 23.4 diffraction signal. Crystallization of the wax on the asphaltene side chains might be occurring at loadings of greater than 1% although it is believed that this would disrupt the aggregation of the asphaltenes to some extent and may lead to better dispersion of the asphaltenes throughout the asphalt

cement but not provide the enhancement reported from (0.8 to 3 % from References 16 and 17). From the insert in the upper right corner of Figure 3.19 the diffraction spectra of the neat Sasobit wax shows that while the diffractions at 2θ = 21.2°and 23.4° are clearly seen, the amorphous band associated with the asphalt cement between ~2θ = 10° and 30° is not in evidence.

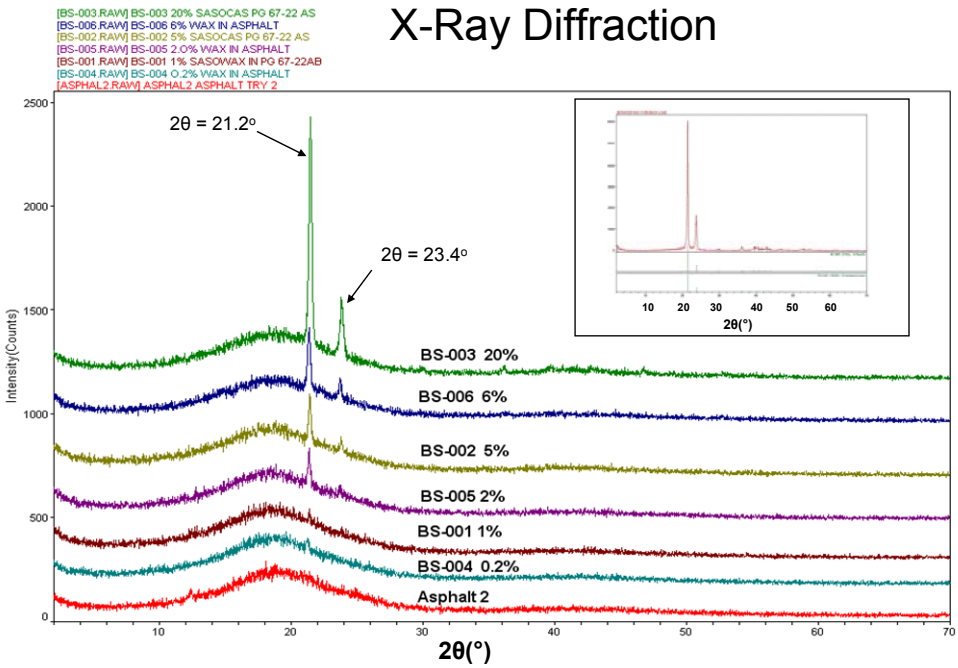

Figure 3.19 The X-ray diffraction patterns for a range of Sasobit in AC loadings

3.4. Epifluorescence Microscopy

Evidence for the room temperature phase-separated structure of Sasobit in asphalt cement can be seen in the 20x magnification slides (Figure 3.20). The upper right image of the neat asphalt cement shows a distinct lack of phase separation within the image (Figure 3.20). This may imply a distinct lack of natural wax crystallization within the neat asphalt cement. The 20 % Sasobit / asphalt cement image shows very

distinct and well distributed phase separation with light colored areas appearing as angular (crystalline) and needle-like in shape(Figure 3.20). If the concept of the Sasobit crystallization occurring on the asphaltene aliphatic side chains is to be believed then the needle-like shape of the crystallites in the image moves this concept more towards plausible as the asphaltene aliphatic side chains could template the structure of the wax crystallizing around it. This fact would also suggest a highly disperse arrangement of the asphaltenes within the sample as it could disrupt the stacked crystalline structure of asphaltenes (Figure 3.16) within the sample. The images of 5 % and 1 % Sasobit / asphalt cement show a decrease in the average size of the crystalline areas within each image and an even distribution of the crystalline areas seems to be evident throughout each image (Figure 3.20). The 1 % Sasobit / asphalt cement is showing a less needle-like and more rounded profile in the phase separated areas (Figure 3.20). This might suggest that the 1 % loading exhibits co-crystallization interaction between the wax and the surrounding asphalt cement and that the asphaltene molecules are able to arrange themselves in a more cross-sectional stacked configuration (Hesp et al. Reference 43).

Epifluorescence microscopy of a 2% Elvaloy / asphalt cement composite (Figure 3.21) compared with neat asphalt cement images clearly show more phase separation on the right 2 % Elvaloy / asphalt cement than the neat asphalt cement left image. These images differ from those previously presented for Sasobit / asphalt cement composites in that there are some very bright point sources of fluorescence as best seen in the left image of Figure 3.21. In the right image these bright point sources of fluorescence have what looks to be thin filament like structures between and dispersed with them.

Figure 3.22 shows the effect of laboratory aging of the Elvaloy/ asphalt cement composite samples with the original (un-aged) composite material image on the left side

and the PAV aged material image on the right. The right image shows larger bright point sources of fluorescence, more clearly separated from each other than the left image but still shows filament - like material attached to the brighter fluorescence sources.

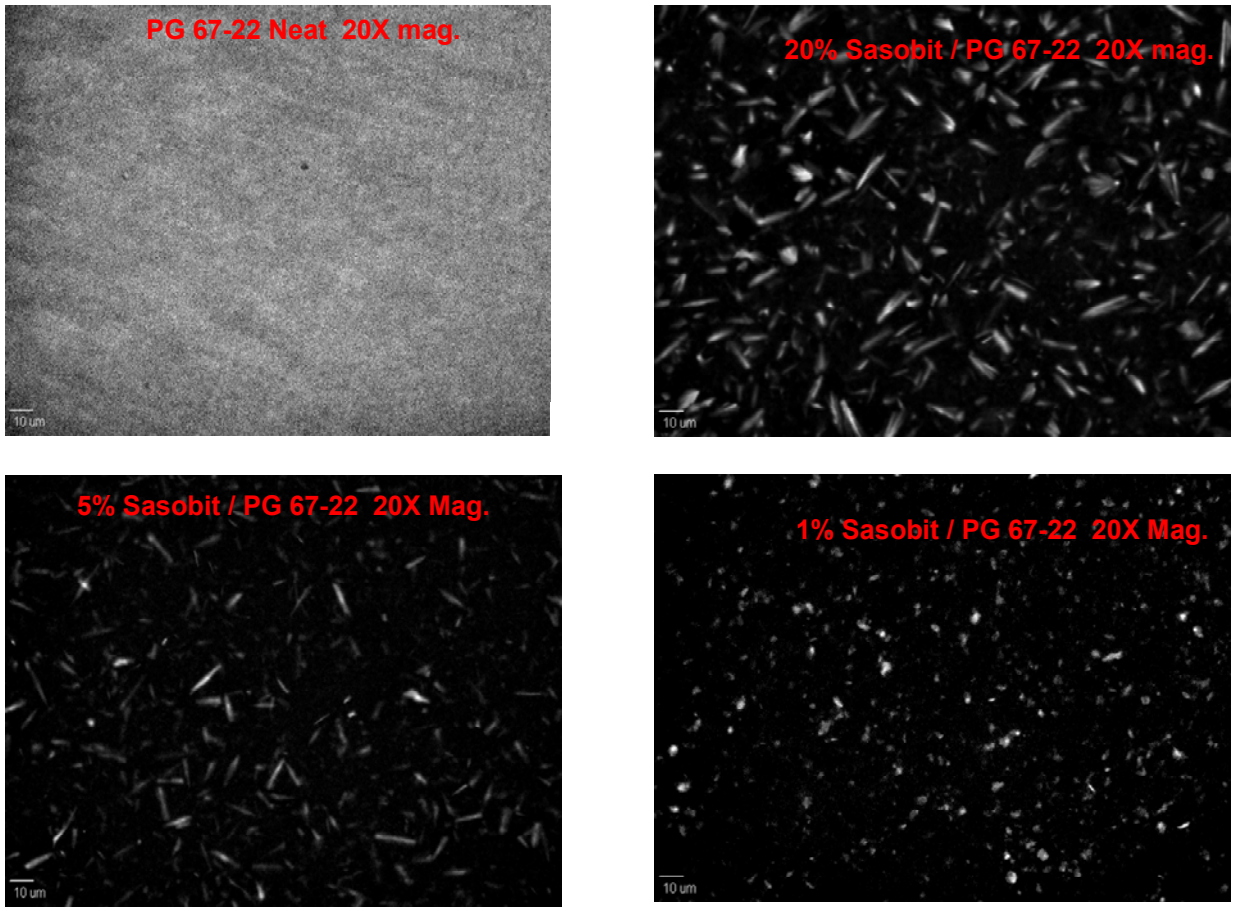

Figure 3.20 Epifluorescence microscopy images of Sasobit/ asphalt cement loadings

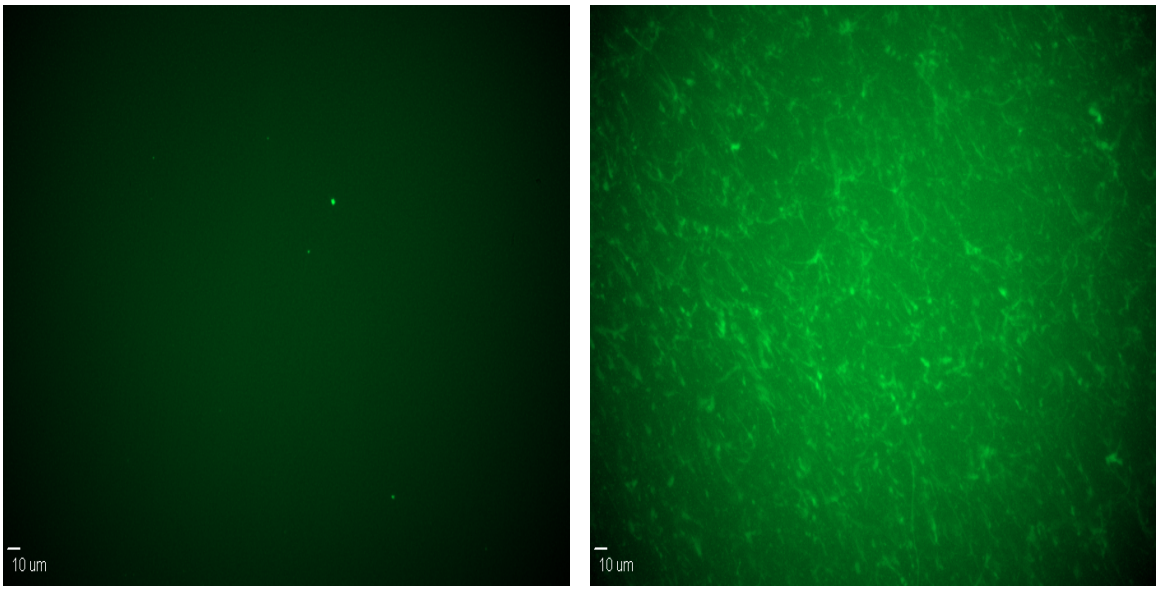

PG 67-22 **2% Elvaloy/ PG 67-22**

Figure 3.21 Original Elvaloy / asphalt cement epifluorescence image compared with original neat asphalt cement epifluorescence image

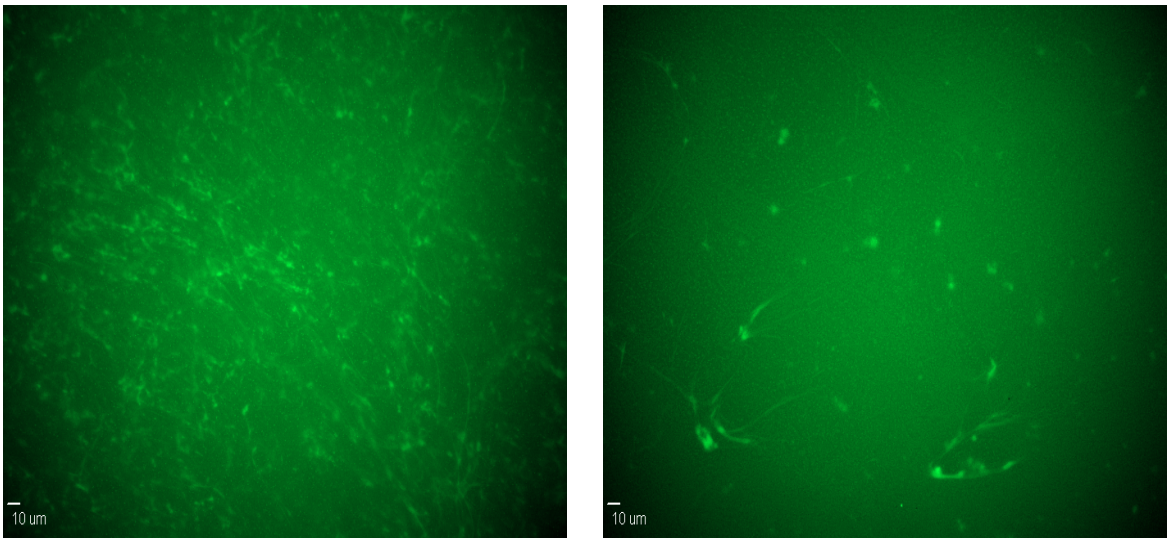

Original material **PAV aged material**

Figure 3.22 Original Elvaloy/ asphalt cement composite epifluorescence image compared with PAV aged epifluorescence image

3.5. Scanning Laser Confocal Microscopy

Bearsley et al. have reported that scanning laser confocal microscopy has been successfully employed to image the asphaltene micelle structures within paving grade asphalt cement samples.[48] They claim that the asphaltene molecules (due to the multi aromatic ring structure) fluoresce between 515–545 nm when excited by a 488 nm laser. They also report that the asphaltene micelles they imaged measured 2–7 μm in size.[48]

Scanning laser confocal microscopy images (Figure 3.23) of the 2 % Elvaloy / asphalt cement composites and changes with PAV aging of the samples were also collected as part of this study. As these images are a combination of slices of the sample area 5 μm into the material surface, scattered fluorescence is greatly eliminated through averaging the slices and the structures producing fluorescence are more clearly shown. As with the previous epifluorescence images (Figures 3.21 and 3.22) of the Elvaloy / asphalt cement composites, we see the bright point sources of fluorescence with filament - like material extending from them in each image.

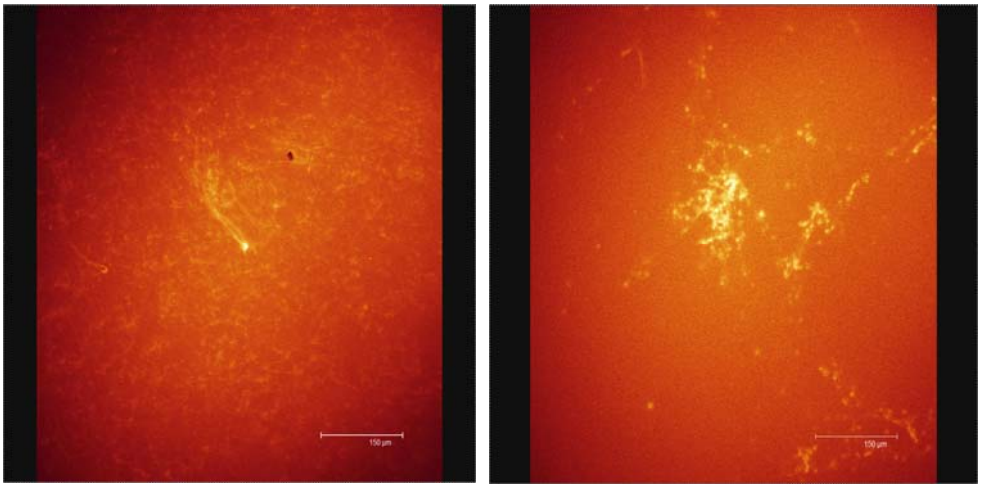

Original material

PAV aged material

Figure 3.23 Original Elvaloy/ asphalt cement composite image compared with PAV aged image (produced through scanning laser confocal microscopy)

In Figure 3.23 the PAV aged image (right) the bright point sources of fluorescence appear closely aggregated with respect to the original material (left).

3.6. Rheology

Since asphalt cement is a colloidal system and exhibits viscoelastic behavior, it can be effectively evaluated through dynamic mechanical analysis (DMA).[2] In DMA, a sinusoidal input of stress or strain is applied to a test specimen and output response is monitored as a function of frequency (ω). Instruments referred to as dynamic shear rheometers utilize geometries such as parallel circular plates to form a test specimen of precise dimension when the test specimen is squeezed between them and excess sample is carefully removed.

Rheology is defined as the science of the deformation and flow of materials.[49] The relationship between shear stress (σ) and strain (γ) or deformation can be related through the shearing modulus (G):[49-51]

$$G = \frac{\sigma}{\gamma}$$

In viscoelastic materials there are two components comprising the complex shearing (G*) modulus, the in-phase (G') storage modulus or elastic component and the out of phase (G") loss modulus or viscous component. Since these two moduli are vectors, the angle (δ) between them will define the elastic and viscous contributions as a vector sum of G*.[49-51]

$$G^* = G' + iG'' \quad \text{and} \quad G^*(\omega) = \sqrt{(G'(\omega))^2 + (G''(\omega))^2}$$

$$\tan\delta = \frac{G''}{G'}$$

There can also be defined a complex viscosity (η*):

$$\eta^* = \eta' - i\eta'' \quad \text{and} \quad \eta''\omega + i\omega\eta' = G' + iG''$$

Where $G' = \eta'' \omega$ and $G'' = \eta' \omega$

Therefore:

$\eta' = \frac{G''}{\omega}$ This is the dynamic viscosity (η')

To produce a master curve one must first develop a series family of rheological data curves such as frequency sweep data evaluated at a set of temperatures. The temperatures chosen must be above a characteristic (T_d) defining temperature for the material such as the glass transition temperature (T_g). The Williams – Landel – Ferry (WLF) equation allows us to reduce the family of single temperature frequency sweep curves to one continuous smooth curve for presentation of data at a chosen temperature over a wide breadth of frequencies through the time-temperature superposition principle.[52] This allows for interpretation of data which cannot readily be collected due to sample testing frequency or instrument limitations.[53] The WLF equation is as follows: [52]

$$\log a(t) = \frac{-C_1(T - T_d)}{C_2 + T - T_d}$$

Where:

a (T) = horizontal shift factor

T = temperature, ^oC of the particular frequency sweep data

T_d = the defining temperature, ^oC

C_1, C_2 = empirical constants.

Anderson et al. have reported that the values of C_1 = -19 and C_2 = 92 are the most appropriate for aged and un-aged SHRP asphalts.[51] Using the TA Instruments – AR2000 DSR and the software package installed, there is a specific TTS algorithm which adjusts the data using the WLF equation and the universal constants C_1 = -17.44

and C_2 = 51.6. TA Instruments' TTS algorithm was used for reducing the data collected from frequency sweeps to form the master curves of data collected for the frequency sweep data collected.

In effort to more clearly present the differences existing between the three frequency sweep master curves sets, a polynomial fit was applied to the 2% Elvaloy Original curve (Figure 3.24) which is represented through the equation of the polynomial fit line. The R^2 value of 0.98677 for this fit indicates that the 2nd degree polynomial function $y = A + B_1x^2 + B_2x$ posted on the figure was a good choice for smoothing the raw data.

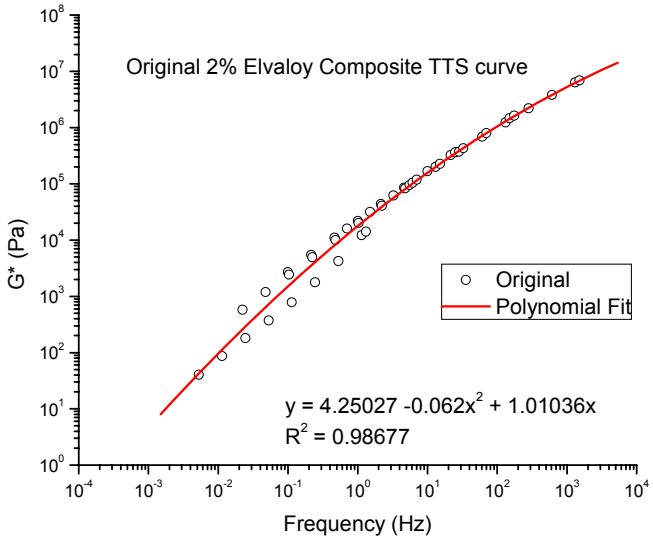

Figure 3.24 Original 2 % Elvaloy composite DSR G* vs. frequency master curves smoothed through polynomial fitting

When such a polynomial fit is applied across the full set of frequency master curves on aging (Figures 3.25 – 3.27) the data point scatter of the "chaotic" region is removed and a smoothed appearance of G^* for each sample is more clearly presented.

Comparison of the G* vs. frequency master curves in Figures 3.25 and 3.26, we see similar behavior in terms of aging response between the PG 64-22 samples and the

Sasobit composites. The 1% Sasobit composite G* curve set is of greater magnitude throughout the frequency decades as expected due loading of the additive mainly to the high molecular mass molecules shown in the GPC-RI chromatogram (Figure 3.6). The TFOT master curve (Figures 3.25 and 3.26) comparison between 1% Sasobit and neat asphalt cement seems to follow the same trend seen in original samples curves. The TFOT aged Sasobit composite curve shows greater overall G* values compared to the neat asphalt cement TFOT curve. The PAV mastercurve comparison (Figures 3.25 and 3.26) between the Sasobit composite and neat asphalt cement samples may suggest that Sasobit provides enhanced long term aging performance with respect to the neat asphalt cement sample. Sasobit inclusion decreases the system viscosity, which allows the asphaltenes more motility while at a temperature above the melting point of Sasobit (as occurs in both TFOT and PAV aging steps). This may be a plausible explanation of the enhancement of G* values in the Sasobit composite compared to the neat asphalt cement sample.

Comparing the PG 64-22 Original sample with the 2% Elvaloy Original sample (Figures 3.25 and 3.27) G* curves, it is apparent that inclusion of the reactive elastic terpolymer has increased the value of G* throughout the frequency range shown. This may be due to the additive's higher molecular mass. This effect increased with aging of the two samples if a comparison is made between the PG 64-22 TFOT with the 2% Elvaloy TFOT G* curves (Figures 3.25 and 3.27). When the PAV curves for these two samples are compared (Figures 3.25 and 3.27), there may be some evidence of crosslinking in the 2% Elvaloy composite between the polymer and asphaltenes or the polymer and itself occurring (Polacco et al. Reference 28). The effect has greatly increased the strength and performance of the Elvaloy composite relative to the PG 64-22 and Sasobit composite samples (Figures 3.25 and 3.27).

To further investigate the difference in rheological behavior across the sample set we look at the changes in the dynamic viscosity curves. Since this experiment was a frequency sweep experiment performed at 30, 40, 50, 60 and 80 ^{o}C and three frequencies per decade, data collection at 1.59 Hz (10 rad/s). 1.59 Hz (10 rad/s) represents the frequency of average traffic on a paving have an average speed of 55 miles per hour. The frequency compared across the sample set is 1 Hz. In their 2004 study to replace the current RTFO aged (G*/sinδ = 2.2 kPa) specification in the PG grading system with η' = 220 Pa*s as a new grading criteria for RTFO aged asphalt cement material, Dongré et al. investigated the performance characteristics of Elvaloy AM modified HMA's and asphalt cement binders.[54]

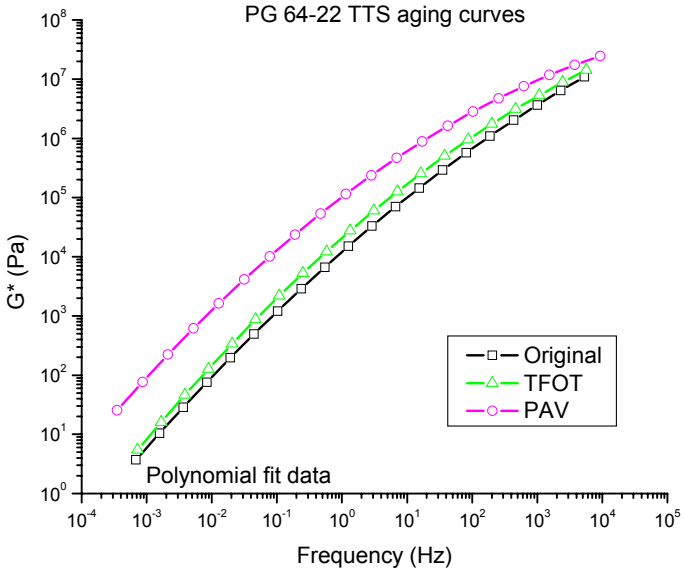

Figure 3.25 Overlay of PG 64-22 DSR G* vs. frequency master curves on aging after polynomial smoothing

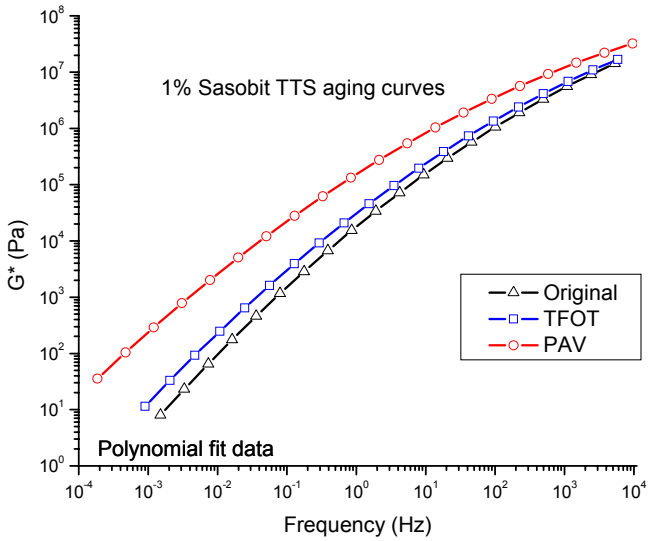

Figure 3.26 Overlay of 1% Sasobit composite DSR G* vs. frequency master curves on aging after polynomial smoothing

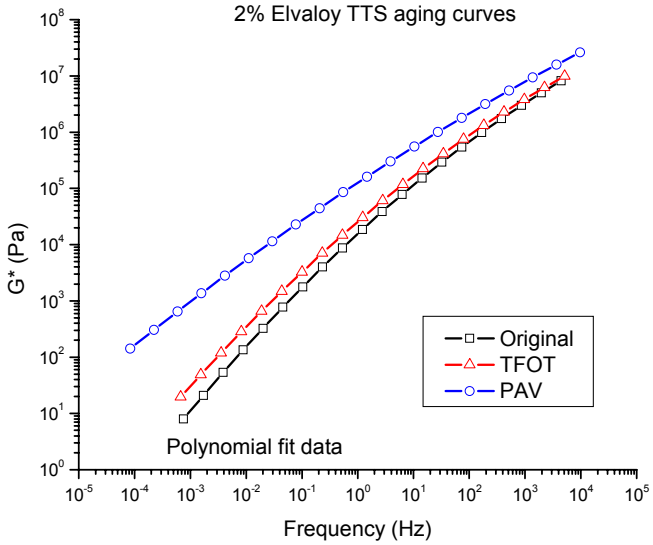

Figure 3.27 Overlay of 2 % Elvaloy composite DSR G* vs. frequency master curves on aging after polynomial smoothing

In the PG 64-22 original sample (Figure 3.28) we see linear behavior of the dynamic viscosity as the sample temperature approaches approximately 54 ^{o}C. Above

54 °C, the dynamic viscosity no longer behaves linearly. This may evidence of system rearrangement to a more expanded system. If the Original PG 64-22 sample (Table 3.3) behaved in a linear fashion one would expect a dynamic viscosity of approximately 13 Pa*s at 80 °C, instead, the measured value is 34 Pa*s. This represents an increase in the system dynamic viscosity of approximately 62 % from a linear response. The DSR values across the sample set are presented in Table 3.6.1. We see negligible % dynamic viscosity difference between the Original PG 64-22 and 1 % Sasobit samples. However, the 2% Elvaloy sample dynamic viscosity closer to linearity that any of the other original samples. TFOT aging (Table 3.3) for PG 64-22 and 1 % Sasobit samples again exhibit approximately equivalent % deviations from linear dynamic viscosity behavior. Comparing PG 64-22 and 1 % Sasobit TFOT samples (Table 3.3) to the 2% Elvaloy sample, the 2% Elvaloy sample shows a relative increase in dynamic viscosity linearity with respect to the other samples. During TFOT aging the samples are strongly heated, it is believed that the heat has caused the Elvaloy AM polymer to plasticize the asphalt cement resulting in closer to linear dynamic viscosity behavior in this system compared to the other samples. Following PAV aging (Table 3.3), all the systems move closer to a linear dynamic viscosity profile with the Sasobit sample exhibiting truly linear dynamic viscosity behavior. The Sasobit composite may have broken up much of viscosity building forces in the system at 80 °C, possibly leading to more even distribution of the asphaltene fraction within the asphalt cement. This evidence lends support to the concept of early stage wax crystalline structure rearrangements (due to the multiple transitions noted in the Chapter 3.2 of this work) on the aliphatic side chains of the asphaltene molecules and improving their molecular mobility within the asphalt cement through reduction of London force attractions.

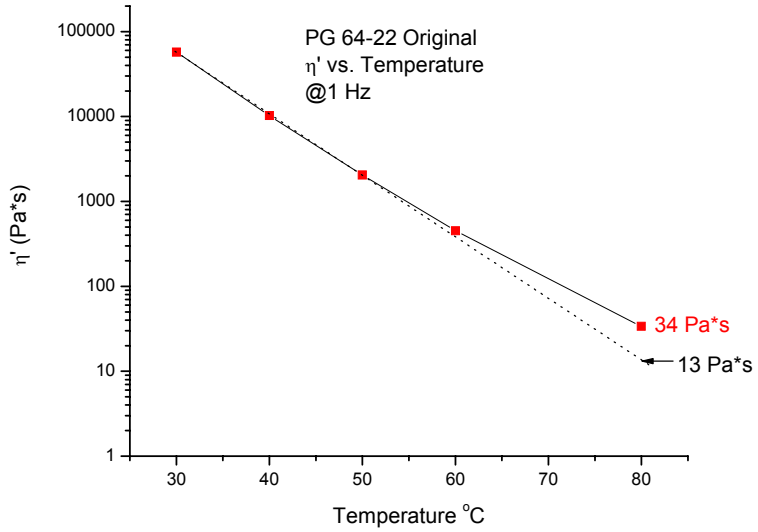

Figure 3.28 The PG 64-22 Original sample DSR chart of η' vs. Temperature

Table 3.3 Deviation from linearity at 80 °C for η' vs. Temperature measured at 1 Hz

Sample	80 °C linear η' value (Pa*s)	80 °C actual η' value (Pa*s)	Δ (%)
PG 64-22 original	13	34	62
PG 64-22 TFOT	27	53	49
PG 64-22 PAV	183	238	23
1 % Sasobit Original	23	64	64
1 % Sasobit TFOT	48	93	48
1 % Sasobit PAV	308	308	0
2 % Elvaloy Original	30	56	46
2 % Elvaloy TFOT	51	111	54
2 % Elvaloy PAV	335	460	27

Note: Charts for PG 64-22 TFOT – 2% Elvaloy PAV appear in the appendix

DSR determination of the PG grade for PG 64-22 original samples and composites was performed and the results appear in (Table 3.4). The temperature at which the value of |G*| / sin (delta) is closest to 1.0 kPa has been defined as the grading temperature. PG 64-22 grades out to PG 70-22 actually, while PG 64-22 / 2% Elvaloy and PG 64-22 / 1% Sasobit grade to PG 76-22. This states that with each of the

composite samples we have increased the PG by one grade through incorporation of the additives at their respective loadings to the asphalt cement and thereby accomplishing significant reinforcement of the composite system.

Table 3.4 DSR PG grading of the PG 64-22 original samples vs. composites

Sample	Temperature	|G*| / sin(delta)
	°C	kPa
PG 64-22 / 2%Elvaloy	58	9.608
	64	4.4
	70	2.118
	76	1.079
	82	0.5798
PG 64-22	58	5.199
	64	2.245
	70	1.035
	76	0.509
PG 64-22 / 1%Sasobit	58	13.47
	64	5.721
	70	2.487
	76	1.139
	82	0.5542

CHAPTER 4

SUMMARY AND CONCLUSIONS

From the GPC-RI data we don't see much difference in the chromatograms of PG64-22 and the 1% Sasobit composites. There is evidence that this additive adds molecular mass to the non - aggregated asphaltene and the aggregated asphaltene components of the asphalt cement but does not clearly increase the molecular mass in these components at a greater rate that the asphalt does without its inclusion. This is likely caused by the negative dn/dc Sasobit response with respect to the asphalt cement dn/dc. The Elvaloy does appear to increase the concentration of the non- aggregated asphaltene and the aggregated asphaltene components in the asphalt cement and this is most evident following PAV aging. The increase in the concentration of the non-aggregated and aggregated asphaltene components is assumed to be due to Elvaloy binding with the asphaltenes (Polacco et al. Reference 28). This effect appears to be accelerated with heating of the composite at temperatures above 100 ^{o}C as is done in the laboratory aging steps.

From the DSC heating curves, Sasobit may co-crystallize with what is believed to be the asphaltene fraction in the asphalt cement at loadings of 0.2 % Sasobit on the mass of the asphalt cement. Evidence of this was seen following 12 hour sample annealing at 40 ^{o}C, with the appearance of two clearly separated endotherms. From integrations of the second heating DSC curve for loadings above 4% Sasobit there appears good agreement between measured ΔH values and calculated ΔH values. The x-ray diffraction data shows a disappearance of the diffraction peak located at $2\theta = 23.4^{o}$ for Sasobit loadings of 2% and greater. This may also be evidence of a co-crystallization occurring within the composite sample at the lower loadings. It could also

be due to the experimental noise overpowering the signal for this loading level and below.

Epifluorescence microscopy images show a marked reduction in crystallite size as the loading of the Sasobit is reduced. The crystalline structures at 1 % loading are distinctly smaller and appear more rounded than the larger and needle-like crystallites found at 5 and 20 % loadings. Evidence of both additives can clearly be seen within the asphalt matrix through epifluorescence and scanning laser confocal microscopy imaging of each of the composite systems investigated. It is believed that these additives capture scattered fluorescence produced in the asphaltenes and act as wave-guides to transmit the collected photons. The bright point sources of fluorescence, most easily picked out in the Elvaloy / asphalt cement images are believed to be asphaltene micelles. The apparent size of the individual asphaltene micelles in these images falls within the 2-7 μm range reported in literature.[48] Evidence of filament -like structures found in Elvaloy AM original composite images may be polymer strands of Elvaloy AM entangled with and dispersed around the asphaltene micelles within the asphalt cement matrix. With PAV aging it is believed that these polymer strands bind with nearby asphaltenes leading to larger networks of covalently bound asphaltenes (Polacco et al. Reference 28). These same asphaltene micelles were not found in the Sasobit / asphalt cement epifluorescence images and are believed to be drowned out by the much greater brightness exhibited by the angular crystallites of Sasobit.

Evidence of improved G* performance in both Sasobit and Elvaloy composite mastercurves with respect to the neat asphalt cement mastercurves has been presented. Although, the Sasobit composite master curves seem to follow the same curve trends seen in the neat asphalt, the difference between the two is seen in the higher Sasobit composite G* values for original, TFOT and PAV data. The dynamic viscosity data at 1 Hz shows that Original and TFOT data doesn't clearly differentiate

Sasobit Composite and neat asphalt cement until the PAV aging. At that stage the Sasobit composite shows truly linear dynamic viscosity response. This may suggest that the Sasobit inclusion to the asphalt has lead to better dispersion of the viscosity building asphaltene component. The Elvaloy composites show better linearity response than the other samples in Original and TFOT dynamic viscosity data. This may be due to a higher degree of softening provided by the polymer inclusion to the material. It is believed that the polymer has experienced some degree of crosslinking following the PAV aging in all the rheological data. The PG grade for original 1 % Sasobit and 2 % Elvaloy composites were found to improve performance by one grade above the un-modified original asphalt cement.

CHAPTER 5

FUTURE RESEARCH

With all of the evidence presented for the concept of Sasobit possibly crystallizing on the asphaltene side chains, one of my future research goals is further investigate through isolating the asphaltene fraction from Sasobit loaded asphalt cement samples. The first step of the Corbett asphalt cement fractionation method may be a way to precipitate the Sasobit / asphaltene fraction. If this doesn't work then a solvent study to find the most appropriate method for Sasobit / asphaltene fraction precipitation should be conducted. Epifluorescence or scanning laser confocal microscopy should be a way to image the precipitated fraction. X-ray diffraction or GPC in THF might also be worth investigating for corroborating evidence of this perceived phenomenon.

The majority of the future research will be devoted to investigation of Elvaloy reinforced asphalt cement composites. The goal will be to determine the impact of Elvaloy AM in PG 64-22 in terms of aging. Samples of the composites will first be made with loadings of 0, 1, 2 and 3 % Elvaloy AM / PG 64-22. These samples will be subjected to GPC, rheology and IR spectroscopy. The GPC in TCB data using an IV detector (with all samples at the same concentration) will give the molecular mass data; multiple shear creep recovery (rheology) will indicate long term performance and stress to failure data. Since Elvaloy AM contains a significant loading of epoxy groups, IR spectroscopy will be performed on the original samples to determine the initial loading of these reactive groups existing in each composite. Solvent extraction schemes will be investigated to determine the best way to separate the Elvaloy polymer from asphalt cement. Various mixtures of solvents will be investigated in pursuit of this goal.

Each of the composites will be subjected to short term aging through TFOT and multiple cycles of PAV for simulation of long term aging. After each of the aging steps,

the material will be subjected to the same battery of analytical techniques as previously described for the original samples. It is hoped that through the monitoring of the rheological changes, changes in various chemical compositions percentage and each composite's mass distribution with aging will reveal the impact of Elvaloy AM in PG 64-22. These aging characteristics will be compared to the data collected from SBS modified asphalt cement samples aged in the same manner.

Polyphosphoric acid has previously been used as a catalyst in cross-linking studies of Elvaloy AM in asphalt cement.[48] A study of crosslinker inclusion to the composites will be performed to determine the optimal loading within the composite samples. Composite samples containing blends of Elvaloy and polyphosphoric acid (at loading greater than catalytic levels) will also be formulated and evaluated as described.

REFERENCES

1) American Society for Testing and Materials. “Standard specification for viscosity-graded asphalt cement for use in pavement construction” ASTM, West Conshohocken, PA ASTM D3381.

2) Roberts, F.L.; Kandhal, P.S.; Brown, E.R.; Lee, D-Y; Kennedy, T.W.; Hot Mix Asphalt Materials, Mixture design and Construction 2nd ed., National Asphalt Pavement Association Research and Education Foundation, Landham, MD, **1996**.

3) American Association for State Highway and Transportation Officials, “Standard specification for performance graded asphalt binder” AASHTO, Washington, DC AASHTO MP1.

4) Leseur, D. “The colloidal structure of bitumen: consequences on the rheology and on the mechanisms of bitumen modification”, *Adv. in Colloid and Interface Sci.*, **2009**, *145*, 42-82.

5) a) Corbett, L.W.; “Composition of asphalt based on generic fractionation, using solvent de-asphaltening, elution-absorption chromatography and densitometry characterization”, *Anal. Chem.* **1969**, *41(4)*, 576-579. b) American Society for Testing and Materials. “Standard test methods for separation of asphalt into four fractions” ASTM, West Conshohocken, PA ASTM D4124

6) Jiang, R.B.; Lin, J.D.; Lin, D.F. “Rheology of asphaltic binders and their effects on asphalt concrete”, *Transp. Res. Rec.*, **1996**, *No. 1535*, 74-80.

7) Brule, B. “Polymer-modified asphalt contents used in the road construction industry: Basic principles”, *Transp. Res. Rec.*, **1996**, *No. 1535*, 48-53.

8) King, G.N.; Harders, O.; Chavenot, P. “Influence of asphalt grade and polymer concentration on the high temperature performance of polymer modified asphalt”, *J. Assoc. Asphalt Paving Technol.*, **1992**, *61*, 29-61.

9) Goodrich, J.L. “Asphalt and polymer modified asphalt properties related to the performance of asphalt concrete mixes”, *J. Assoc. Asphalt Paving Technol.*, **1988**, *57*, 116-75.

10) Mohammad, L.N.; Negulescu, I.I.; Wu, Z.; Daranga, C.; Daly, W.H.; Abadie, C. "Investigation of the use of recycled polymer modified asphalt binder in asphalt concrete pavements", *J. Assoc. Asphalt Paving Technol.* **2003**, *72*, 551-94.

11) Mohammad, L.N.; Negulescu, I.I.; Daly, W.N. "Evaluation of Warm Mix Asphalt Technology in Flexible Pavements", LA BOR LEQSF, Proposal (7/01/2006 – 6/30/2009).

12) Cooper, S.D.; Mohammad, L.N.; Saadeh, S. "Evaluation of HMA mixtures containing Sasobit", Louisiana Transportation Research Center – Technical Assistance Report 06-1TA (6/2006).

13) Hurley, G.C.; Prowell, B.D. "Evaluation of potential processes for use in warm mix asphalt", *J. Assoc. Asphalt Paving Technol.* **2006**, *75*, 41-90.

14) http://www.fhwa.dot.gov/pavement/asphalt/wma.cfm

15) http://www.meadwestvaco.com/Products/MWV002106

16) http://www.sasolwax.com/Sasobit_Technology.html

17) http://www.sasolwax.com/data/sasolwax_/Bitumen%20Modification/Sasobit%20since%201997.pdf

18) Kanitpong, K.; Nam, K.; Martono, W; Bahia, H. U. "Evaluation of a warm-mix additive", *Construction Materials* **2008**, *161*, 1-8.

19) American Society for Testing and Materials. "Standard specification for hot-laid bituminous paving mixes", ASTM, West Conshohocken, PA ASTM D3515

20) Bahia, H.U.; Friemel, T.P.; Peterson, P.A., Russell, J.S.; Poehnelt, B. "Optimization of constructability and resistance to traffic: a new design approach for HMA using the Superpave compactor", *J. Assoc. Asphalt Paving Technol.* **1998**, *67*, 189-232.

21) American Society for Testing and Materials. "Standard test method for effect of moisture on asphalt concrete paving mixtures" ASTM, West Conshohocken, PA ASTM D4867.

22) Mallick, R.B.; Kandhal, P.S.; Bradbury, R.L. “Using Warm-Mix asphalt technology to incorporate high percentage of reclaimed asphalt pavement material in asphalt mixtures”, *Transp. Res. Rec.*, **2008**, *No. 2051*, 71-79.

23) Mallick, R.B.; Bradley, J.E.; Bradbury, R.L. “Evaluation of heated reclaimed asphalt pavement material and wax-modified asphalt for use in hot mix asphalt”, *Transp. Res. Rec.*, **2007**, *No. 1998*, 112-22.

24) Edwards, Y.; Tasdemir, Y.; Issacson, U. “Rheological effects of commercial waxes and polyphosphoric acid in bitumen160/220 – low temperature performance”, *Fuel.* **2006**, *85*, 989-97.

25) Edwards, Y.; Tasdemir, Y.; Issacson, U. “Effects of commercial waxes asphalt concrete mixtures performance at low and medium temperatures”, *Cold Reg. Sci. Technol.* **2006**, *45*, 31-41.

26) Krupa, I.; Mikova, G.; Luyt, A.S. “Phase change materials based on low-density polyethylene / paraffin wax blends”, *Eur. Polym. J.* **2007**, *43*, 4695-705.

27) http://www2.dupont.com/Elvaloy/en_US/products/elvaloy_asphalt_modifiers.html

28) Polacco, G.; Stasta, J.; Biondi, D.; Antonelli, F.; Vlachovicova, Z.; Zanzotto, L. “Rheology of asphalts modified with glycidylmethacrylate functionalized polymers”, *J. Colloid Interface Science* **2004**, *280*, 366-73.

29) Yildirim, Y. “Polymer modified asphalt binders”, *Constr. Build. Mater.* **2007**, *21*, 66-72.

30) Bhurke, A.S.; Shin, E.E.; Drzal, L.T. “Fracture morphology and fracture toughness of polymer - modified asphalt concrete”, *Transp. Res. Rec.*, **1997**, *No. 1590*, 23-33.

31) Khattak, M.J.; Baladi, G.Y.; Drzal, L.T. “Low temperature binder-aggregate adhesion and mechanistic characteristics of polymer modified asphalt mixtures”, *J. Mater. Civil Eng.*, **2007**, *No. 1998*, 112-22.

32) American Society for Testing and Materials. “Test method for effect of heat and air on asphaltic materials”, ASTM, West Conshohocken, PA ASTM D1754.

33) American Society for Testing and Materials. “Standard practice for accelerated aging of asphalt binder using a pressurized aging vessel”, ASTM, West Conshohocken, PA ASTM D6521.

34) Sperling, L.H., “Introduction to physical polymer science”, **2001**, John Wiley and Sons, Inc. New York, NY

35) http://chem.chem.rochester.edu/~chem421/propsmw.htm

36) Luyt, A.S., Krupa, I “Thermal behavior of low and high molecular weight paraffin waxes used for designing phase change materials”, *Thermochim. Acta* **2008**, *467*, 117-20.

37) Hammami, A.; Mehrotra, A.K. “Thermal-behavior of polymorphic *n*-alkanes - effect of cooling rate on the major transition-temperatures”, *Fuel* **1995**, *74*, 96-101.

38) Ungar, G.; Masic, N. “Order in the rotator phase of normal-alkanes” *J. Phys. Chem.* **1985**, *89*, 1036-42

39) Severtson, S.J.; Nowak; M.J. “Molecular restructuring kinetics and low-velocity wetting of n-alkane rotator phases by polar liquids”, *Langmuir* **2002**, *18*, 9371-76.

40) Genovese, A; Amarasinghe, G.; Glewis, M.; Mainwarring, D.; Shanks, R.A. “Crystallization, melting, re-crystallization- and polymorphism of *n*-eicosane for application as a phase change material”, *Thermochim. Acta* **2006**, *443*, 235-44.

41) Daly, W.H.; Qiu, Z.; Negulescu, I.I. “Differential scanning calorimetry study of asphalt crystallinity”, *Transp. Res. Rec.*, **1996**, *No. 1535*, 54-60.

42) Masson, J-F.; Polomark, G.M. “Bitumen microstructure by modulated differential scanning calorimetry”, *Thermochim. Acta* **2001**, *374*, 105-14.

43) Hesp, S.A.M.; Serban, I.; Shirokoff, J.W. “Reversible aging in asphalt binders”, *Energy Fuels* **2007**, *21*, 1112-21.

44) Bouhadda, Y.; Bormann, D.; Sheu, E.; Bendedouch, D.; Krallafa, A.; Daaou, M. “Characterization of Algerian Hassi-Messaoud asphaltene structure using Raman spectroscopy and x-ray diffraction”, *Fuel* **2007**, *86*, 1855-64.

45) Siddiqui, M.N.; Ali, M.F.; Shirokoff, J.W. “Use of x-ray diffraction patterns in assessing the aging pattern of asphalt fractions”, *Fuel* **2002**, *81*, 51-58.

46) Shirokoff, J.W.; Siddiqui, M.N.; Ali, M.F. “Characterization of the structure of Saudi Crude asphaltenes by x-ray diffraction”, *Energy Fuels* **1997**, *11*, 561-65.

47) Lu, X.; Redelius, P. “Composition and structural characterization of waxes isolated from bitumen”, *Energy Fuels* **2006**, *20*, 653-66.

48) Bearsley, S.; Forbes, A.; Haverkamp, R.G. “Direct observation of asphaltene structure in paving-grade bitumen using confocal laser-scanning microscopy”, *J. Microsc.* **2004**, *215 (2)*, 149-55.

49) Rosen, S.L., “Fundamental principles of polymeric materials”, 2nd ed., **1993**, John Wiley and Sons, Inc., New York, NY

50) Anderson, D.A.; Christensen, D.W., Bahia, H.U. “Physical properties of asphalt cement and the development of performance-related specifications”, *J. Assoc. Asphalt Paving Technol.* **1991**, *60*, 437-75.

51) Christensen, D.W., Anderson, D.A. “Interpretation of dynamic mechanical test data for paving grade asphalt”, *J. Assoc. Asphalt Paving Technol.* **1992**, *61*, 67-98.

52) Williams, M.L., Landel, R.F., and Ferry, J.D., “The temperature dependence of relaxation mechanisms in amorphous polymers and other glass-forming liquids”, *J. of Am. Chem. Soc.* **1955,** 77, 3701-06.

53) Daranga, C., “Characterization of aged polymer modified asphalt cements for recycling purposes”, Ph. D. Dissertation, **2005**, Department of Chemistry, Louisiana State University, Baton Rouge, LA.

54) Dongré, R.; D’Angelo, J.D.; Reinke, G. “New criterion for Superpave high-temperature binder specification”, *Transp. Res. Rec.*, **2004**, *No. 1875*, 22-32.

APPENDIX: SUPPLEMENTARY DATA

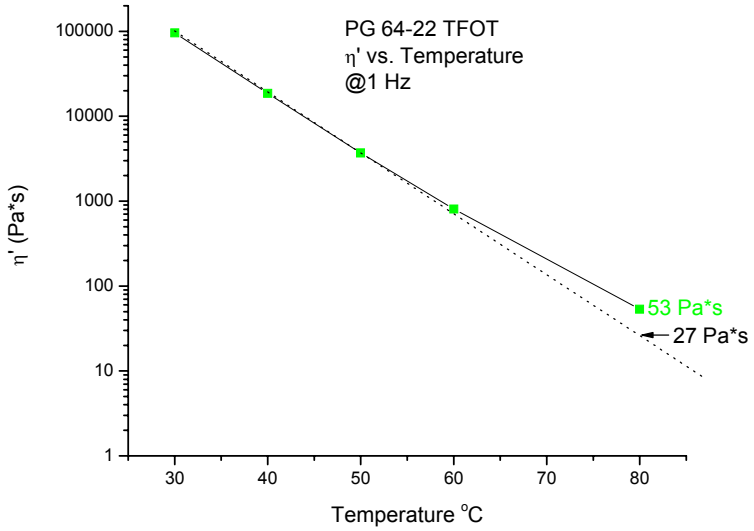

Figure A.I PG 64-22 TFOT sample DSR chart of η' vs. Temperature

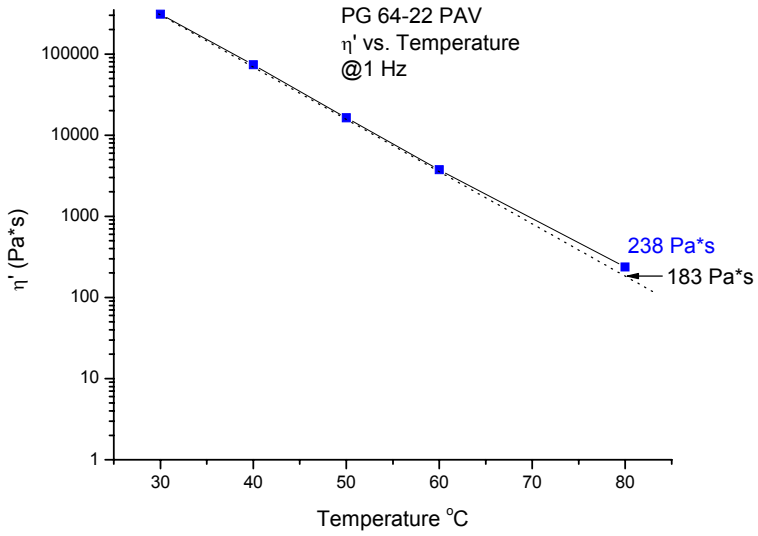

Figure A.2 PG 64-22 PAV sample DSR chart of η' vs. Temperature

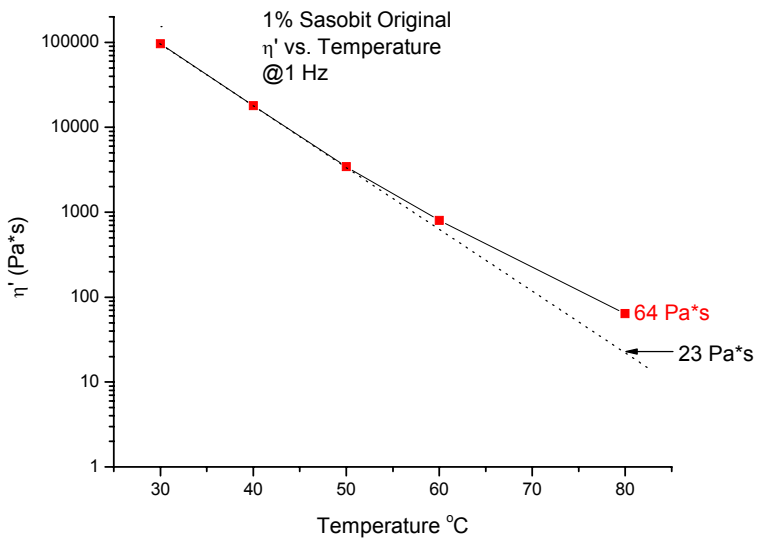

Figure A.3 Original 1 % Sasobit sample DSR chart of η' vs. Temperature

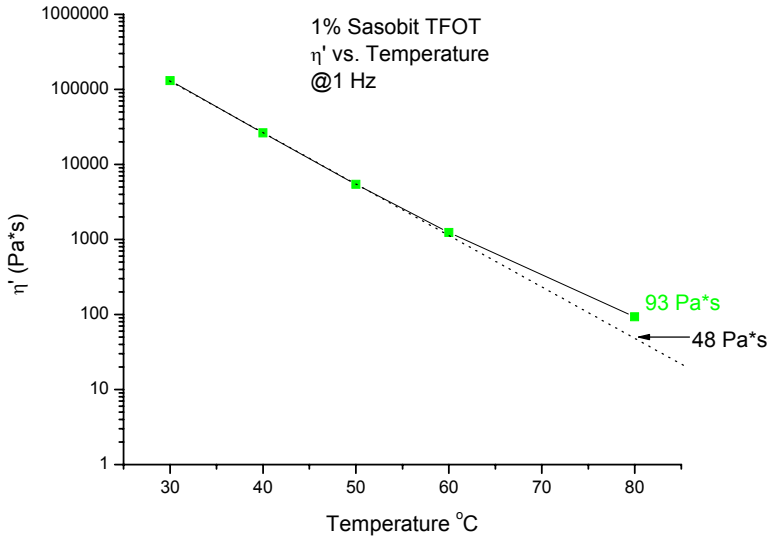

Figure A.4 TFOT 1 % Sasobit sample DSR chart of η' vs. Temperature

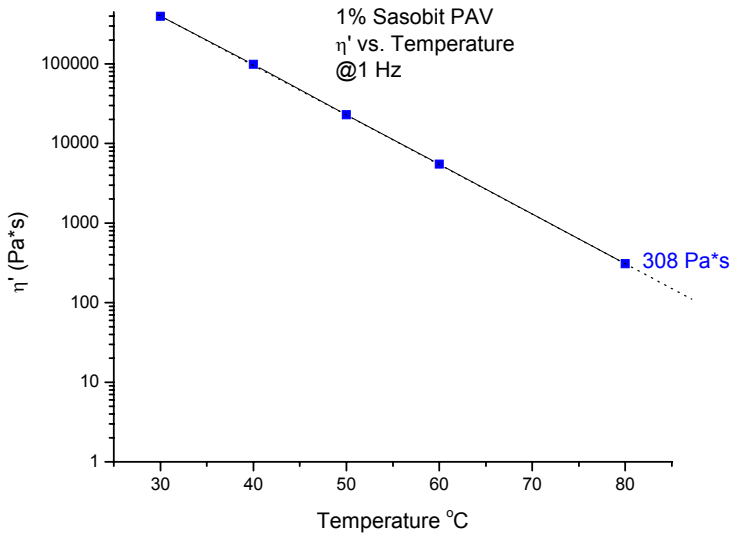

Figure A.5 PAV 1 % Sasobit sample DSR chart of η' vs. Temperature

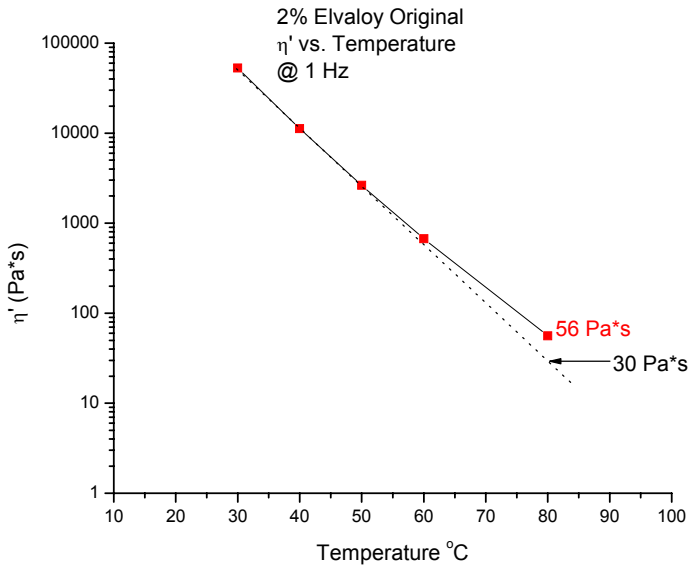

Figure A.6 Original 2 % Elvaloy sample DSR chart of η' vs. Temperature

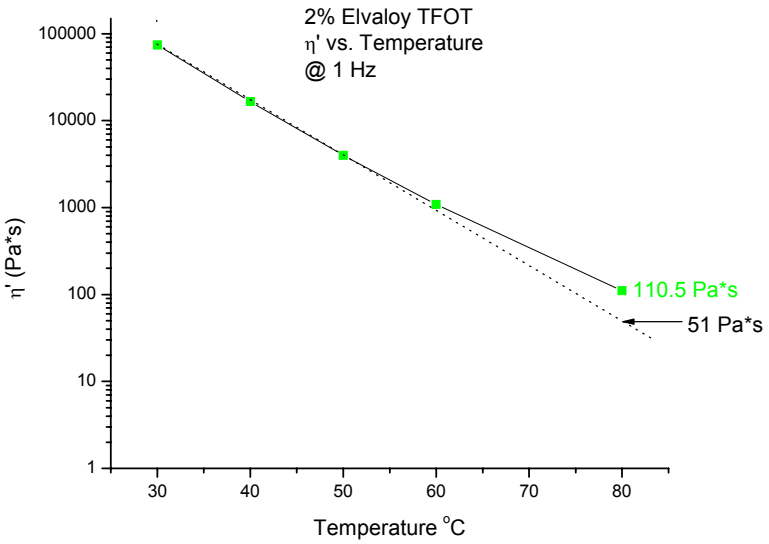

Figure A.7 TFOT 2 % Elvaloy sample DSR chart of η' vs. Temperature

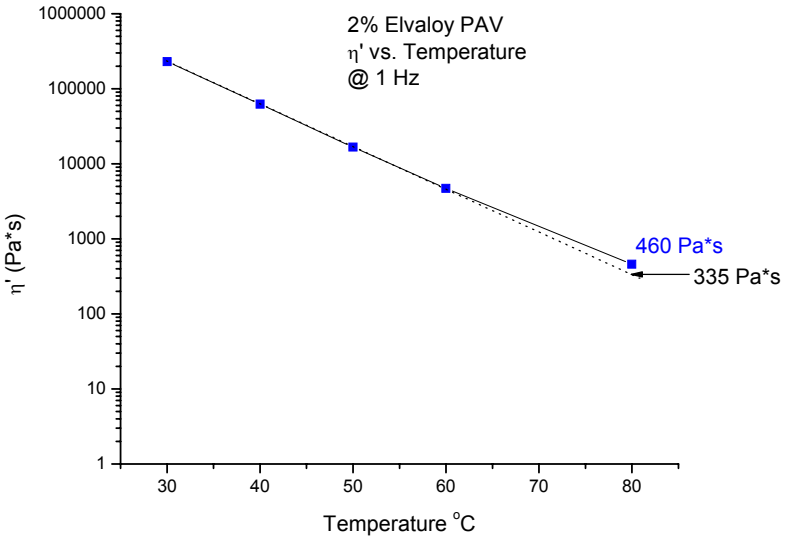

Figure A.8 PAV 2 % Elvaloy sample DSR chart of η' vs. Temperature

VITA

Brent H. Sellers was born in Pensacola, Florida. He is the son of Edward D. and Ruth L. Sellers. Brent graduated with a Bachelor of Science degree, cum laude, from the University of North Carolina at Charlotte in 1999. His interest was in Polymer Science and the industrial applications of a wide range of polymers. In 2000, he accepted a position as a Development Chemist within the Pressure Sensitive group of the Adhesives division at National Starch and Chemical Company in Bridgewater, New Jersey. Under the direction and mentorship of Paul B. Foreman, PhD, he performed solvent borne free - radical synthesis of hybrid - acrylic base polymers and formulation of a variety of solvent and water borne adhesive compounds. While at National Starch and Chemical Company he enrolled in the New Jersey Institute of Technology Graduate School and received a Graduate Certificate in Polymer Chemistry in 2003. He also worked as a Research and Development Chemist for the Main Tape Company in Cranbury, New Jersey. Brent was accepted by the Louisiana State University Graduate School as a graduate student in the Department of Chemistry and subsequently joined Professors William H. Daly and Ioan I. Negulescu as a member of their research group. His investigations focused on characterization of performance additive modified asphalt cements through a variety of techniques. During this period he became familiar with the concepts of Civil Engineering related to asphalt cement design and asphalt pavement construction through the invaluable guidance of Professor Louay N. Mohammad and the staff of the Louisiana Transportation Research Center.